**Regulation of Notch signaling by a chromatin modeling protein Hat-trick**

Ankita Singh, Maimuna S Paul, Debdeep Dutta, Mousumi Mutsuddi*, Ashim Mukherjee*

Department of Molecular and Human Genetics,
Institute of Science,
Banaras Hindu University,
Varanasi-221005,
Uttar Pradesh, India

*Corresponding Authors
Email: ashim04@gmail.com
mousumi_mutsuddi@yahoo.com

Keywords: Cell Signaling, Notch, activation complex, *Enhancer of Split* complex, Chromo-domain, *hat-trick*, *Drosophila*

## Summary statement

Hat-trick is a novel interactor of Notch which genetically interacts with Notch pathway components. Our results demonstrate that Htk is a component of Notch-Su(H) activation complex and hence positively regulates Notch signaling.


## Abstract

Notch signaling plays pleiotropic role in astounding variety of cellular processes including cell fate determination, differentiation, proliferation and apoptosis. The increasingly complex regulatory mechanisms of Notch signaling account for the multitude of functions exhibited by Notch during development. We identified Hat-trick (Htk), a DNA binding protein, as an interacting partner of Notch-ICD in a yeast two-hybrid screen and their physical interaction was further validated by co-immunoprecipitation experiments. *htk* genetically interacts with Notch pathway components in trans-heterozygous combinations. Loss of *htk* function in *htk* mutant somatic clones showed down-regulation of Notch targets, whereas over-expression of *htk* caused ectopic expression of Notch target, without affecting the level of Notch protein. Immunocytochemical analysis has demonstrated that Htk co-localizes with over-expressed Notch-ICD in the same nuclear compartment. We have shown here that Htk cooperates with Notch-ICD and Suppressor of Hairless to form activation complex and binds to the regulatory sequences of Notch downstream targets, *Enhancer of Split* complex genes to direct their expression. Taken together, our results suggest a novel mode of regulation of Notch signaling by a chromatin modeling protein Htk.

## Introduction

Notch signaling is an evolutionary conserved pathway that regulates a wide variety of developmental processes including acquisition of specific cell fates, cell proliferation, differentiation, self-renewal and cell death programs (Cabrera, 1990; Egan et al., 1998; Artavanis-Tsakonas et al., 1999; Fehon et al., 2007; Fortini, 2009; Liu et al., 2010; Andersson et al., 2011; Guruharsha et al., 2012). Notch is subjected to tight regulation at the level of receptor and ligand biosynthesis, post-translational modifications, ligand-receptor interaction and its trafficking. The intricate regulatory mechanisms of Notch signaling account for the diverse functions of same pathway in numerous cellular contexts during development of an organism (Baron et al., 2002). The Notch receptor is synthesized as a 300kDa single polypeptide precursor which gets cleaved by furin-like convertase(s) during maturation in the trans-Golgi network. N-terminal extracellular subunit and a C-terminal transmembrane intracellular subunit join through a non-covalent bond to form a single transmembrane hetero-dimeric receptor that translocates to the cell membrane (Blaumueller et al., 1997; Logeat et al., 1998). Notch signal transduction is initiated when Notch receptor interacts with its ligands, Delta and Serrate (*Drosophila)* from its neighboring cells (Rebay et al., 1991), and initiates proteolytic cleavage by ADAM (A Disintegrin And Metalloprotease domain) /TACE (TNFα Converting Enzyme) /Kuzbanian family of metalloproteases (Brou et al., 2000; Mumm et al., 2000). This cleavage between the extracellular domain and transmembrane domain generates a membrane tethered Notch, Notch extracellular truncation (NEXT) fragment which is subsequently cleaved by the γ-secretase complex (De Strooper et al., 1999; Struhl and Greenwald, 1999; Ye et al., 1999). This cleavage results in the release of Notch-intracellular domain (Notch-ICD/NICD) which eventually translocates to the nucleus with the help of Importin-α3 molecule (Sachan et al., 2013). In the nucleus Notch-ICD binds to and activates a transcription factor, Suppressor of Hairless in *Drosophila* (CBF1/RBPJ in vertebrates) and displaces the co-repressors and recruits co-activators, including Mastermind leading to activation of Notch target genes (Fortini and Artavanis-Tsakonas, 1994; Struhl and Adachi, 1998; Wu et al., 2000; Cau and Blader, 2009). In *Drosophila*, the majority of Notch target genes identified so far is positioned in the Enhancer of split complex [E(spl)]. E(spl) is a complex locus containing, among others, seven transcription units, *m8*, *m7*, *m5*, *m3*, *mβ*, *mγ*, and *mδ*, which encode basic helix-loop-helix (bHLH) transcriptional repressors (Delidakis and Artavanis-

Tsakonas, 1992; de Celis et al., 1996; Bray and Furriols, 2001). This complex of genes is often regulated by Notch signaling and is critically important for neurogenesis and in making cell-fate decisions.

In order to identify novel regulators of Notch-ICD, a yeast two-hybrid screen was performed and we identified *Drosophila* Hat-trick (Htk) as an interacting partner of Notch-ICD. Htk is a DNA binding protein that harbors ARID, Chromo-domain and Tudor-domain (Figure 1A). These domains are present in proteins which are involved in DNA binding and chromatin modeling (Herrscher et al., 1995; Iwahara, and Clubb, 1999; Akhtar et al., 2000; Brehm et al., 2000; Bouazoune et al., 2002; Iwahara et al., 2002; Kim et al., 2006). Beside the sequence homology with chromatin remodeling proteins, Htk is also reported to interact with the histone deacetylase, Sin3A protein (Spain et al., 2010). We have recently shown its role in mediating important chromatin functions such as karyosome structure, DSBs repair, etc., during *Drosophila* oogenesis (Singh et al., 2018). Based on following evidence, Htk is presumed to be a chromatin modeling protein, however its functional characterization is not yet complete. It has derived its name from its putative role in heterochromatinization and its influence on TDP-43 mediated toxicity (Sreedharan et al., 2015). The gene *htk* encodes two annotated transcript variants which could be translated into two polypeptides of size 186 kDa and 259 kDa, respectively. Bioinformatic analysis revealed that Htk can regulate transcription from RNA polymerase II promoter (Gaudet et al., 2010). The mammalian orthologs of Htk, ARID4A and ARID4B, are members of the chromatin-remodeling complex and function as transcriptional repressors upon recruitment by tumor suppressor RB, hence are also known as RB-binding protein1 (RBBP1, RBP1) and RBBP1-like protein 1 (RBBP1L1), respectively (Defeo-Jones et al., 1991; Lai et al., 1999; 2001; Cao et al., 2001; Fleischer et al., 2003).

In present study, we characterized the functional significance of Notch and Htk interaction. We have carried out experiments to propose that Htk is a part of Notch-Su(H) activation complex. Using molecular and genetic analyses, we found that Htk acts as positive regulator Notch signaling. Our co-immunoprecipitation experiments reconfirmed their physical interaction. *htk* also showed genetic interactions with components of Notch signaling pathway. Loss-of-function and gain-of-function studies revealed its pleiotropic role in regulating several developmental events. Several phenotypes generated by loss or gain of *htk* function mimicked Notch mutant

phenotypes that further gave a hint towards the role of *htk* as a modulator of Notch signaling. Over-expression of *htk* leads to up-regulation of Notch signaling as evident by ectopic expression of Notch target Cut without changing the level of Notch-ICD in the developing wing imaginal discs. Conversely, Notch targets Cut and Wingless were down-regulated in *htk* mutant clones, indicating *htk* to be a positive regulator of Notch signaling. Additionally, we observed that Htk protein co-localizes with expressed Notch-ICD in the same nuclear compartment. Further, it was observed that Htk can immunoprecipitate Su(H), a transcription factor of Notch signaling. The fragments of regulatory sequences of Notch targets, E(spl) complex genes, were chromatin-immunoprecipitated with Htk, confirming that Htk is a component of regulatory complex. Real time analysis of E(spl) complex genes expression from *htk* over-expressed tissue confirmed that Htk is a part of activation complex. Thus, our functional analyses indicate Htk to be a novel modulator of Notch signaling in *Drosophila.*

## Results

### Htk is an interacting partner of Notch

In a yeast two-hybrid screen, we identified Htk as an interacting partner of Notch. In the same screen, multiple positive clones of Suppressor of Hairless, a well-established binding partner of Notch-ICD, were also identified, which validates our approach. Amino terminus of Notch-ICD (amino acids 1765–1895) was used as a bait to screen $6x10^6$ cDNAs from a *Drosophila* 0–24 h embryonic library. Eleven positive clones ($His^+$) were isolated and found to encode overlapping *htk* cDNAs. Sequence analysis of overlapping domain revealed that the carboxy-terminal part of Htk (amino acids 2424–2486), which is very specific to the protein, is sufficient for binding to Notch-ICD (Figure S1A).

Co-immunoprecipitation experiments further validated the physical interaction of Notch with Htk. Using extracts from wing discs co-expressing HA-tagged Htk and Notch-ICD, we demonstrated that Htk or Notch could be immunoprecipitated with either anti-HA or anti-Notch antibodies (Figures 1B, 1C). Moreover, expressed HA-Htk was able to co-immunoprecipitate endogenous Notch (Figure 1D). We also observed that endogenous Htk was sufficient to immunoprecipitate Notch from larval salivary gland when only Notch-ICD was over-expressed (Figure 1E).

Immunocytochemical analysis further revealed that endogenous Htk [marked by Anti-Htk antibody, generated previously in the lab (Singh et al., 2018)] and over-expressed Notch-ICD co-localized in the same nuclear compartment (Figures 1F-1Q).

### *htk* genetically interacts with Notch pathway components

To further analyze the functional implications of the physical interaction between the Htk and Notch proteins, we investigated whether mutations in *htk* and *Notch* pathway components display genetic interactions in trans-heterozygous combinations. Three *htk* loss-of-function alleles, $htk^{71}$, $htk^{49}$, and $htk^{37}$, were used for genetic interaction studies. Both *Notch* and *htk* genes are located on I chromosome and their null alleles are hemizygous lethal, thus it was not possible to check the genetic interaction between them in trans-heterozygous condition. A trans-heterozygous combination of a *htk* allele and a dominant negative allele of Notch (*UAS-Notch-DN*) resulted in an enhancement of wing nicking phenotype, indicating a further decrease of Notch function (Figures 2A-2D). We found an enhanced wing nicking phenotype when different *htk* alleles were brought in combination with the Suppressor of Hairless gain-of-function allele, *Su(H)T4* (Figures 2E-2H, S1B), and loss-of-function allele, *Su(H)1* (Figures 2I-2L, S1B). Suppressor of Hairless (Su(H)) is a DNA-binding protein component of the Notch signaling pathway and its gain-of-function or loss-of-function should result in reduced Notch signaling activity, as Su(H) is a component of both repression as well as activation complex (Furriols and Bray, 2000). Earlier it has been clearly shown that excess Su(H) can compete with the normal Su(H) and Notch-ICD containing activation complex and free Su(H) alone can bind to the DNA which leads to inactivation of some downstream Notch target genes that require both Su(H) and Notch-ICD for their activation (Furriols and Bray, 2000). Thus, we believe that similar to the case of Su(H) loss-of-function alleles, when we reduced the dosage of *htk* along with heterozygous Su(H) gain-of-function allele, there was a further reduction of Notch signaling as shown by increased wing nicking phenotype in both the cases. *C96-GAL4*-driven expression of dominant-negative, C-terminal Mastermind (Mam) truncation display fully penetrant wing-nicking phenotype (Figure 2M) (Helms et al., 1999; Kankel et al., 2007). Reducing the dose of *htk* in these individuals elicited enhanced wing notching phenotype (Figures 2M-2P). Our genetic interaction screen displayed that, different *htk* loss-of-function mutants when combined with Notch pathway mutants further

reduced the Notch signaling activity, resulting in more severe phenotypes. We note that *htk* mutants showed a strong genetic interaction with the transcription factors and co-activators involved in Notch signaling pathway.

### *htk* loss-of-function results in downregulation of Notch signaling without any alteration of Notch protein levels

We generated *htk* mutant somatic clones in larval wing imaginal discs using different *htk* loss-of-function mutant alleles and FLP-FRT system (Xu and Rubin, 1993). In $htk^{71}$ mutant clones, no significant change in the Notch protein level was observed in comparison to the surrounding wild-type cells (Figures 3A-3A'''). Furthermore, we checked the status of Notch signaling activity by looking at the expression level of downstream targets of Notch, Cut and Wingless. It has been shown that Notch induces Cut and wingless expression at the dorso-ventral (DV) boundary of developing wing disc (Neumann and Cohen, 1996). Here we observed that protein levels of both Cut and Wingless were significantly reduced in $htk^{71}$ mutant clones compared to wild type sister cells at DV boundary region (Figures 3B-3D'''). In addition, we also observed that the expression of a Notch signaling reporter, NRE-GFP was significantly reduced in *htk* loss-of-function clones (Figures 3E-E'''). Adults carrying *htk* clones displayed Notch loss-of-function phenotypes such as wing notching and increased scutellar bristle phenotypes (Figures S5G, S5H). Thus, loss of Htk resulted in reduced Notch signaling activity without affecting the level of Notch receptor.

### Over-expression of Htk modulates Notch signaling activity

We further examined the influence of ectopic expression of *htk* on Notch expression and its localization. HA-tagged *htk* was over-expressed in the anterior-posterior margin of wing disc using *ptc-GAL4* driver and it was observed that expression of HA-Htk did not affect the level or localization of the endogenous Notch protein (Figures 4A-4C). Next, we investigated the level of Notch signaling activity by checking the status of Cut, which expresses under the influence of Notch signaling at the DV boundary of wing disc (Neumann and Cohen, 1996). Whereas over-expression of *HA-htk* at the anterior-posterior boundary of the wing discs resulted in ectopic expression of Cut along the AP junction of the pouch region within the wing disc (Figures 4D-4I).

**Loss-of-function and gain-of-function of *htk* renders wing and eye phenotypes similar to Notch mutant phenotypes**

As seen in imaginal discs, we also observed down-regulation and gain-of-function effects of *htk* in adult tissues using various tissue specific GAL4 drivers (Brand and Perrimon, 1993) (Figures S1C, S1D). *htk-RNAi* was used to see the tissue specific loss-of-function effects of *htk*. However, this RNAi stock caused a weak RNA interference and as a result variability in expressivity and incomplete penetrance was observed. Down-regulation of *htk* in dorsal region of wing discs which makes adult thorax and wing, using *apterous-GAL4,* resulted in increased scutellar bristles (Figures S2C, S2D) and wings were bent outward and upward probably due to thorax muscle defects (Figure S2A, S2B). These wings also had extra rows of bristles (Figure S2G). *htk* down-regulation, using *patched-GAL4* driver, in anterior-posterior boundary resulted in reduction of intervein distance between L3-L4 veins and reduced first cross-vein (Figure S2F). *dpp-GAL4* driven down-regulation of *htk* also resulted in extra vein material and sometimes an extra cross-vein at anterior-posterior boundary region (Figure S2I). Further, loss of *htk* at wing margin using *C96-GAL4* resulted in extra vein material, and areas with thinner cuticle at or near wing margin (Figure S2J). *MS1096-GAL4* driven *htk-RNAi* also showed the similar phenotypes (data not shown). *engrailed-GAL4* driven *htk-RNAi* resulted in thinner wing blade in posterior region of wings (Figure S2K). Thus, loss of *htk* in different regions of wings resulted in extra vein material, extra bristles and small patches of disorganized tissues phenotypes (Figures S2H-H”). Loss of *htk* in eye using *eyeless-GAL4* resulted in loss of ommatidia and reduced eye size (Figure S2L). Most of these *htk* down-regulation phenotypes also correspond to Notch loss-of-function phenotypes. It is well established that Notch is needed for the wing margin, veins, and sensory bristles development and loss of Notch also results in reduced inter-vein distance and reduced eye size (Hartenstein and Posakony, 1990; Go and Artavanis-Tsakonas, 1998; Casso et al., 2010).

Additionally, HA-tagged *htk* was over-expressed in different regions of wing discs and eye discs, using various tissue specific GAL4 drivers. Gain-of-function of HA-Htk in dorsal region of wing discs, using *apterous-GAL4* driver, resulted in loss of scutellar bristles and reduced size of scutellum and severe wing blisters (Figure S3B-S3D). Over-expression in posterior region of wing discs using *engrailed-GAL4* resulted in bending of third wing vein, thinner wing blade and incomplete fifth vein (Figure S3H). *HA-htk* gain of function in eye using *GMR-GAL4* and *eyeless-*

*GAL4* drivers resulted in eye roughening (Figures S3J, S3L) and loss of ommatidia (Figure S3F), respectively. A few of these observed phenotypes are very similar to Notch gain-of-function phenotypes such as loss of bristles, loss of vein material and increase in eye roughening phenotypes (Hartenstein and Posakony, 1990; Go and Artavanis-Tsakonas, 1998; Casso et al., 2010).

**_htk_ shows epistatic interaction with _Notch_ and _Su(H)_ and it is required for Notch-Su(H)-mediated downstream target gene expression**

To determine the epistatic interaction of *htk* with *Notch* or *Su(H)*, we examined whether *htk* can rescue loss or gain-of-function phenotypes of *Notch* or *Su(H)*. A severe wing notching phenotype was caused by reduction of Notch signaling when *Notch-RNAi* (*NIRM*) was expressed at the wing margin (Figures S4A). It was observed that wing nicking phenotype was significantly rescued when HA-tagged *htk* was over-expressed in this background (Figures S4B). In the opposite direction, over-expression of *Notch-ICD* or *Su(H)VP16* at wing margin driven by *C96-GAL4* resulted in irregular wing margin bristles (Figures S4C-S4E). This irregular bristle phenotype was significantly rescued by decreasing the expression of *htk* using *htk-RNAi* in the same background (Figures S4H-S4J, S4V-S4W). Thus, it was observed that overexpression of *htk* can rescue the wing phenotypes caused by *Notch* loss-of-function and reduction of *htk* expression leads to rescue of gain-of-function effects of *Notch* and *Su(H)VP16* in the wing margin (Figures S4A-S4J, S4V-S4W).

Additionally, when we co-expressed *HA-htk* along with *Notch-ICD* or *Su(H)VP16* at wing margin using *C96-GAL4* driver, we observed an increase in the wing margin irregularities which reflected a synergistic behavior of *htk* with *Notch* and *Su(H)VP16* (Supplemental Figures S4M- S4O).

We further confirmed the epistatic interaction by looking at the expression of Notch downstream target, Cut (Neumann and Cohen, 1996). Loss of Cut expression was observed when *Notch-RNAi* was expressed at dorso-ventral boundary of wing disc using *C96-GAL4* driver (Figures S4Q). The reduced activity of Notch signaling, as seen by reduction of Cut expression, was partially rescued when *HA-htk* was expressed in the same background (Supplemental figure S4R, S4X). On the other hand, reducing the expression of *htk* using *htk-RNAi* partially rescued the ectopic Cut expression caused by over-expression of *Su(H)VP16* at dorso-ventral boundary of wing disc using *C96-GAL4* line (Figures S4T-S4U, S4Y).

To further confirm the role of Htk in Notch-Su(H) mediated downstream target gene expression, we over-expressed *Notch-ICD* or *Su(H)VP16* in *htk* mutant clonal cells using the MARCM technique (Lee and Luo, 2001). In *UAS-Notch-ICD* and *UAS-Su(H)VP16* lines, *Notch-ICD* and *Su(H)VP16* are under *UAS* promoter and the *tub-GAL4* was used to drive *Notch-ICD* and *Su(H)VP16* globally, but the presence of *GAL80* inhibited *GAL4*-induced expression of *Notch-ICD* and *UAS-Su(H)*VP16 in all cells except in those cells in which *GAL80* was eliminated due to *FLP-FRT* mediated somatic recombination events. In the same mutant clonal cells, *htk* gene function was also eliminated at the same time. As a result, these *Notch-ICD* and *Su(H)VP16* over-expressing clonal cells, which were also marked with GFP, were mutated for *htk* gene. In parallel, MARCM analysis of wild-type clones without *htk* mutation was also carried out. The status of Notch downstream target, Cut was examined in the clonal cells. Without *htk* mutation *Notch-ICD* and *Su(H)VP16* expressing clones showed ectopic Cut expression (Figures 5A-5D, 5I-5L). Interestingly, in absence of *htk*, *Notch-ICD* and *Su(H)VP16* could not show its complete activity and a reduction in ectopic Cut expression was observed in these mutant clonal cells (Figures 5E-5H, 5M-5P).

In addition to MARCM analysis, *Su(H)VP16* was over-expressed at dorso-ventral boundary using C96-*GAL4* driver in a separate set of experiments and in this background FLP-FRT-mediated *htk* null clones were generated. Many of these *htk* null clones also showed similar results displaying reduction of ectopic Cut expression (Figures 5Q-5T). All these results confirmed that *htk* is required for complete Notch signaling activity, and *NICD* or *Su(H)* cannot execute its complete function in the absence of *htk*.

**Htk is a component of Notch activation complex**

Immunocytochemical analysis revealed that endogenous Htk and over-expressed Notch-ICD co-localized in the same nuclear compartment (Figures 1F-1I). These two proteins overlapped in the inter-chromatin and chromatin space within the nucleus (Figures 1J-1M). It has been established that Notch forms an activation complex in the nucleus to express downstream target genes (Fortini and Artavanis -Tsakonas, 1994; Struhl and Adachi, 1998; Borggrefe and Oswald, 2016). We aimed to check whether Htk is a component of Notch-ICD activation complex in nucleus. Co-

immunoprecipitation experiment with HA-tagged Htk revealed that HA-Htk was able to pull down Su(H) when Htk and Notch-ICD were co-expressed in larval wing discs (Figure 6A). Additionally, we also observed that HA-Htk is sufficient to immunoprecipitate endogenous Su(H) when only endogenous Notch was present (Figure 6A). This confirmed that Htk and Su(H) belong to the same activation complex. We have also reported above that Htk physically interacts with Notch-ICD (Figure 1). Thus, we conclude that Htk is a component of Notch-Su(H) transcription complex.

We further wanted to explore the mechanism of regulation of Notch signaling by *htk*. Nuclear localization, DNA binding ability and its physical interaction with Notch-ICD prompted us to hypothesize that Htk might bind to the promoter sequences of Notch targets and co-operate with Notch-ICD for the activation of these downstream targets. To validate our hypothesis we did Chromatin Immunoprecipitation (ChIP) of expressed HA-tagged Htk using HA beads followed by PCR using primers (Figures S5J) for promoter sequences of well-established Notch targets, *E(spl)* complex genes. The Chromatin Immunoprecipitation (ChIP) is a potent technique to identify the *in vivo* association of transcription factors with regulatory elements. We observed that indeed the Htk binds to the promoter sequences of Notch target genes (Figure 6B). To further confirm that Htk is a component of activation complex and not the repressor complex, we observed the status of two of these *E(spl)* complex genes, *E(spl)m8* and *E(spl)mβ*, in *htk* loss-of-function clones and we also analysed expression of seven *E(spl) bHLH* transcripts in *HA-htk* over-expressed background. The *LacZ* reporter stocks were used to verify their expression which was indeed down-regulated in *htk* loss-of-function clones (Figures S5A-S5F). Furthermore, when we checked the real-time expression of these targets, we found an increase in expression of *E(spl)* complex genes with the increase in Htk expression (Figure 6C), confirming our hypothesis that Htk is an important component of Notch co-activation complex. Thus, we show that Htk interacts with the Notch ICD and is recruited to promoters of Notch target genes to activate their expression (Figure 6D).

## Discussion

Notch signaling pathway has been used to regulate a variety of cellular processes. Despite the plethora of information about this conserved signaling pathway, the intricate regulatory mechanism of Notch activation is far from complete. Here we report for the first time that chromatin modeling protein Htk is a novel interactor of Notch-ICD. Htk is a Chromo, ARID and Tudor domain containing protein and these domains renders this protein a putative DNA binding activity. Htk protein was identified as an interacting partner of Notch-ICD in a yeast two hybrid screening; we present evidence that Htk physically interacts with the Notch-ICD and shows genetic interaction with mutants of Notch pathway components especially with the components of transcription factor complex. Htk is a nuclear protein and co-localizes with the expressed Notch-ICD inside the nucleus. Our loss-of-function and the complementary gain-of-function analyses indicate that Htk in involved in the regulation of Notch signaling. We present evidences that Htk is a component of Notch activation complex. In absence of Notch signaling CSL [CBF-1/RBPJ in vertebrates, Su(H) in *Drosophila melanogaster*, lag-1 in *Caenorhabditis elegans*] remain associated with repressor complex and actively represses transcription of target genes. Upon activation of Notch signaling, CSL binds to Notch-ICD and displaces the CSL-associated repressor complex and recruits co-activators, and consequently leads to transcriptional activation of Notch target genes (Fortini and Artavanis -Tsakonas, 1994; Struhl and Adachi, 1998). Based on different experimental evidences it has been predicted that CSL mediated transcription of downstream target genes becomes switched on or off depending on molecular signature on the chromatin created by associated activator or repressor complexes, respectively [Borggrefe and Oswald, 2016; Giaimoa et al., 2017). Surprisingly the DNA binding affinity of CSL is extremely low. There is no evidence to show either co-repressor complex binding or Notch-ICD-activator complex binding to CSL has any impact to its DNA-binding affinity. It was speculated that other DNA binding protein in the CSL activator complex may facilitate its chromatin association (Giaimoa et al., 2017). Our results present here clearly show that DNA binding protein Htk is present in the Su(H) activator complex and consequently it leads to the activation of transcription of target genes such as E(Spl) complex genes. Epistasis analysis confirmed that Notch-ICD and Su(H) require Htk to execute its complete function. We presume that association of DNA-binding protein Htk in Notch-ICD-Su(H) activator complex stabilizes and sustains the binding of Su(H) with DNA and as a result transcriptional

activation of Notch target genes takes place. Thus, our results establish a novel mode of regulation of Notch signaling by a chromatin modeling protein Htk.

Recent reports revealed that Sin3A physically binds with Htk (Spain et al., 2010), and also with its human homologue ARID4A and ARID4B (Lai et al., 2001; Fleischer et al., 2003; Suryadinata et al., 2011; Wan et al., 2015). Histone deacetylase Sin3A, acts as a negative regulator of transcription (Silverstein and Ekwall, 2005; Kadosh and Struhl, 1998). Sin3A is a binding partner of Su(H), and is a part of transcription repressor complex involved in suppression of Notch target gene expression in absence of Notch protein (Zhou et al., 2000). However, here we established that Htk is involved in transcription activation complex to turn on the Notch downstream target gene expression in presence of Notch protein. The exact role of Htk in regulating the switch from repressor to activation complex is yet to be determined, At this point we can predict that like Su(H), Htk may also be present in both the repressor and activator complex and it may be required to stabilize and sustains the binding of Su(H) to the promoter sequences of Notch downstream target genes in both the complexes.

The data presented here describe Htk as a positive regulator of the Notch signaling pathway in *Drosophila*. Htk has been previously reported to interact with repressor genes such as Sin3A (Spain et al., 2010), and the mammalian orthologs of Htk, ARID4A and ARID4B, are members of the chromatin-remodeling complex and function as transcriptional repressors in different contexts (Patsialou et al., 2005). Contrary to this, we show that loss-of-function of Htk decreases Notch signaling and gain-of-function of Htk leads to upregulation of Notch activity, suggesting a transcriptional activator function of Htk in regulating the Notch pathway. This is not the first report showing positive regulation of Notch signaling by a repressor protein. According to a recent report a well-established transcriptional repressor protein, the histone deacetylase HDAC1 acts as a positive regulator of Notch signaling (Wang et al., 2018). It has been shown that HDAC1 along with the HDAC1-associated transcriptional co-repressor Atrophin (Atro) regulates Notch protein levels by promoting Notch transcription (Wang et al., 2018). Similarly, our results also reveal a previously unidentified transcriptional activator function of a predicted repressor complex protein Htk in regulating Notch downstream target gene expression during development.

Similar to CSL in Notch signaling activation, switching from repression to activation function of transcription factor was also observed in other signaling pathways such as TCF/LEF (T-cell factor/lymphoid enhancer factor) in Wnt signaling pathway. Htk may play very similar function in these signaling pathways and the spectrum of Htk function remains to be explored. Being a chromatin binding protein, Htk can be speculated to regulate the expression of wide range of genes during development. Thus, it would be worth to explore its function in regulating the activity of different signaling pathways, including Wnt, Hippo, JNK, Hh, etc.

Notch-Htk interaction may have several functional implications in regulating a spectrum of cellular processes. Recently it has been revealed that loss of *htk* suppresses TDP-43-mediated age-dependent neurodegeneration seen in amyotrophic lateral sclerosis (ALS) (Sreedharan et al., 2013). Accumulation of nuclear RNA-binding protein TDP-43 (encoded by the TARDBP gene) in the cytoplasm is the histopathologic signature of degenerating neurons in ALS. Earlier, investigations on gene expression patterns that accompany TDP-43-induced neurotoxicity in *Drosophila* system have shown strong up-regulation of cell cycle regulators and Notch target genes (Zhan et al., 2013). It has also been shown that mutations in Notch pathway components extended lifespan of TDP-43 transgenic lines (Zhan et al., 2013). Thus, Notch activation has deleterious effect in TDP-43 flies. Since Sreedharan group has already reported that *htk* mutations have been seen to suppress TDP-43 toxicity, it is very tempting to speculate that Htk may play an important role in activation of Notch signaling which leads to the TDP-43 mediated neurodegeneration in ALS. Thus, Htk may have a potential to be considered as future therapeutic target for ALS therapy.

## Materials and Methods

### Yeast Two-hybrid

A 393bp *Drosophila* Notch cDNA (accession number M11664) fragment which encodes amino acids 1765–1895 containing NLS was cloned in frame with the sequence encoding the LexA DNA-binding domain of bait vector. This construct was used as bait to screen oligo(dT)-primed *D. melanogaster* 0–24 h embryo cDNA libraries cloned in pGAD prey vectors containing GAL4 activation domains. A yeast two-hybrid screen was carried out as described previously (Mukherjee et al., 2005). Sequencing was performed for all positive pGAD plasmids from *His*+ colonies.

## Immunoprecipitation and immunoblotting

For co-immunoprecipitation Notch-ICD was over-expressed in larval salivary glands under the control of *sgs-GAL4* driver. Salivary glands were dissected and homogenized in lysis buffer [25Mm Tris, pH 8.0, 27.5mM NaCl, 20mM KCl, 25mM sucrose, 10mM EDTA, 10mM EGTA, 1 mM DTT, 10% glycerol, 0.5% Tergitol solution, 1 mM PMSF, and 1X protease inhibitor (Roche)]. Crude lysate containing 3 mg of total protein was mixed with 5µl of anti-Htk antibody and 20 µl of protein A/G beads and kept for an end-over-end rotator for overnight at 4 °C. No antibody was added in controls samples. Beads were collected after washing three times with lysis buffer and separated on 12% denaturing SDS polyacrylamide gel and transferred onto Immuno-Blot PVDF membranes (Bio-Rad). After washing for 10 min in TBST [Tris base (50mM), NaCl (150mM), Tween-20 (0.1%)], and blocking (4% skimmed milk in TBST) for 30min, blots were probed with mouse anti-Notch antibody (C17.9C6, 1:3000 dilution, Developmental Studies Hybridoma Bank). Again after washing three times in TBST and another blocking for 30 min, goat anti-mouse IgG-AP conjugate in 1:2000 dilution (Molecular Probes) in blocking solution was added for 90 min followed by three washings in TBST. Color was detected by Sigma FAST BCIP/NBT (Sigma).

Similarly, lysates were prepared from larval wing disc expressing Notch-ICD and HA-Htk , and only HA-Htk using *vg-GAL4* driver, followed by immunoprecipitation with anti-HA affinity beads (Sigma), and anti-Notch antibody along with A/G beads. We used monoclonal mouse anti-Notch (C17.9C6) antibody at dilution 1:3000 for detection of Notch, and mouse anti-HA antibody at 1:1000 dilution (Sigma) for detection of HA, and Rabbit anti-Su(H) antibody at 1:1000 dilution (Santa Cruz). Secondary antibody, Goat anti-mouse IgG-AP conjugate or anti-rabbit IgG-AP conjugate in 1:2000 dilution (Molecular Probes) were used.

## *Drosophila* genetics

All fly stocks were maintained on standard corn meal/ yeast/ molasses/ agar medium at 25°C. Oregon-R flies were used as wild-type controls. *htk* null mutant alleles, $htk^{71}$ *FRT19A/FM7*, $htk^{39}$ *FRT19A/FM7,* and $htk^{47}$ *FRT19A/FM7* were kindly provided by Jemeen Sreedharan (Sreedharan *et al*., 2015). Notch pathway components were kindly provided by S. Artavanis-Tsakonas. We used the following stocks for our studies:

For genetic interaction: *C96-GAL4, UAS-Dominant negative Notch* (*UAS-DNN7*), *Su(H)T4* (Gain-of-function allele), *Su(H)1* (loss-of-function allele) (BL417), *C96-GAL4, UAS-MamH.*

For epistatic studies: *UAS-Notch-RNAi* (*UAS-NIRM*), *UAS-Su(H)VP16* (II) (provided by Sarah Bray), and *UAS-Su(H)VP16/TM3 ser* (provided by Jessica Treisman).

For loss-of-function and Gain-of-function studies: *UAS-htk-RNAi* (BL31574), *UAS-Notch-RNAi*, *NRE-eGFP* (BL30728) and *UAS-HA-htk* (Fly Line ID: F000657). *UAS-HA-htk* stock was ordered from FlyORF, Zurich (it expresses functional but truncated form of Htk protein).

GAL4 driver lines: *en-GAL4, C96-GAL4, Sgs3-GAL4, ap-GAL4, MS1096-GAL4, vg-GAL4, ptc-GAL4, ey-GAL4* and *GMR-GAL4* were ordered from Bloomington Stock Centre.

For mosaic generation: *hs-FLP neoFRT19A Ubi-RFP* (BL31418), *neoFRT19A* (BL1709)
To generate somatic clones, we used the FLP/FRT system. Males of *hs-FLP neoFRT19A Ubi-RFP* strain was crossed with $htk^{71}$ *FRT19A/FM7,* $htk^{47}$ *FRT19A/FM7* and $htk^{39}$ *FRT19A/FM7* females. Heat shock was given at 37 °C for 60 min at 24 hr after egg laying (AEL), and the third instar female larvae were analyzed for mutant clones. We observed similar phenotypes in all the *htk* alleles, therefore we have shown results only for $htk^{71}$ mutation as a representative one.

To generate MARCM-derived clones *and* $htk^{71}$ mutant clones in *Su(H)VP16* over-expression background, following flies were generated by appropriate genetic crosses -
*hs-FLP neoFRT19A Ubi-RFP/Y; +/+; C96-GAL4*
*hs-FLP neoFRT19A tub-GAL80/Y; +/+; tub-GAL4 UAS-GFP/TM6c sb*
$htk^{71}$ *FRT19A/FM7; UAS-Su(H)VP16*
$htk^{71}$ *FRT19A/FM7; UAS-NICD*
*neoFRT19A/FM7; UAS-Su(H)VP16*
*neoFRT19A/FM7; UAS-NICD*

The MARCM system was used to generate GFP-marked $htk^{71}$ mutant clones over-expressing *Notch-ICD* or *Su(H)VP16*. Females of $htk^{71}$ *FRT19A/FM7; UAS-Su(H)VP16* and $htk^{71}$ *FRT19A/FM7; UAS-NICD* were crossed to males *hs-FLP neoFRT19A tub-GAL80/Y; +/+; tub-GAL4 UAS-GFP/TM6c sb*. In parallel, a control experiment was carried out in which females of *neoFRT19A/FM7; UAS-Su(H)VP16* and *neoFRT19A/FM7; UAS-NICD* were used for crosses.

Heat shock was given at 37°C for 60 min at 24 hrs AEL and third instar female larvae were analyzed for GFP-marked clones.

To generate *htk*$^{71}$ mutant clones in *Su(H)VP16* over-expression background, *hs-FLP neoFRT19A Ubi-RFP/Y; +/+; C96-GAL4* was crossed with *htk*$^{71}$ *FRT19A/FM7; UAS-Su(H)VP16* (experimental) and *neoFRT19A/FM7; UAS-Su(H)VP16* (Control). Rest of the procedure was same as mentioned above.

**Eye imprints**

Eye imprints using nail polish were made for analyzing ommatidial defects, and were examined under differential interference contrast (DIC) optics in a Nikon Eclipse Ni microscope.

**RNA isolation, semi quantitative and quantitative real-time PCR**

Total RNA was isolated using Trizol method from imaginal discs of third instar larvae. Single stranded cDNA was prepared using reverse transcriptase (NEB) after DNAse treatment. This CDNA was used as a template DNA for semi-quantitative and real-time PCR. qPCR was carried out as per the manufacturer's protocol (Applied Biosystem). A total of 10 µl of the reaction volume included 5 µl 2× SYBR green, 0.25 µl each forward and reverse primer, and 1 µl cDNA, and PCR was performed using ABI 7500 instrument. Data were normalized to *rps17* before calculating the relative fold change.

Primers for RT PCR

mβ_RT_Fw 5'- ACCGCAAGGTGATGAAGC -3'

mβ_RT_Re 5'- CTTCATGTGCTCCACGGTC -3'

mδ_RT_Fw 5'- ATGGCCGTTCAGGGTCAG -3'

mδ_RT_Re 5'- CCATGGTGTCCACGATG -3'

mγ_RT_Fw 5'- GTCCGAGATGTCCAAGAC -3'

mγ_RT_Re 5'- GACTCCAAGGTGGCAACC -3'

m3_RT_Fw 5'- ATGGTCATGGAGATGTCC -3'

m3_RT_Re 5’- GCACTCCACCATCAGATC -3’

m5_RT_Fw 5’- ATGGCACCACAGAGCAAC-3’

m5_RT_Re 5’-TGTCCATTCGCAGGATGG -3’

m7_RT_Fw 5’- GGCCACCAAATACGAGATG -3’

m7_RT_Re 5’- CAT CGC CAG TCT GAG CAA -3’

m8_RT_Fw 5’- GGAATACACCACCAAGACC -3’

m8_RT_Re 5’- CGCTGACTCGAGCATCTC -3’

**Immunostaining of imaginal discs**

For immunostaining imaginal discs from third instar larvae were dissected in cold phosphate buffered saline (PBS). It was followed by 20 min incubation in 4% paraformaldehyde. Tissues were then washed four times in washing solution (a mixture of 1×-PBS, 0.2% Triton-X-100 and 0.1% bovine serum albumin) for 10 min each followed by incubation in blocking solution (Tri-PBS with 0.1% BSA and 8% normal goat serum) for 60 min. Primary antibodies were diluted in blocking solution, added to the ovaries and incubated overnight at 4 °C. After four washes in washing solution and 60 min blocking, secondary antibodies were added in 1:200 dilution, incubated for 90 min at room temperature. It was followed by four washes in washing solution for 15 min each. DAPI (49, 6-diamidino-2-phenylindole dihydrochloride) (1µg/ml) was added for 20 min to the tissues after a PBS wash. After final dissection in cold PBS, samples were then mounted in DABCO. The following primary antibodies were used- Rabbit polyclonal anti-Htk (1:100) (Singh et al., 2018), anti-Notch raised in mouse (1:300) (C17.9C6), mouse anti-Wg (1:100) (4D4), mouse anti-Cut (1:100) (2B10) from Developmental Studies Hybridoma Bank (DSHB), mouse anti-HA (1:100) from Sigma, mouse anti-βGAL (1.5:100) from Promega. Secondary Antibodies used were: Alexa Fluor 555 conjugated goat anti-mouse IgG (1:200), Alexa Fluor 488 conjugated goat anti-mouse IgG (1:200), Alexa Fluor 555 conjugated goat anti-rabbit IgG (1:200), Alexa Fluor 555 conjugated goat anti-rat IgG (1:200) and Alexa Fluor 488 conjugated goat anti-rabbit IgG (1:200) from Molecular Probes.

Fluorescent images were obtained with a Carl Zeiss LSM780 confocal microscope.

**Chromatin immunoprecipitation (ChIP)**

100 heads were dissected from *GMR-GAL4, UAS-HA-htk* flies in 1X PBS and fixed in 1% formaldehyde solution at RT for 20 min. Incubation for 1 min in 0.125 M glycine solution was done to stop cross-linking followed by three times washing in 1X cold PBS. 400 µl of nuclear lysis buffer (1% SDS, 10 mM EDTA, 50 mM Tris-HCl, pH 8, 1X Protease inhibitor) was added and heads were homogenized followed by sonication (QSonica, Q700) (50 cycles, amplitude at 90, pulse on 30 sec, pulse off 1min). After centrifuge supernatants (chromatin samples) were collected and stored in -20°C. DNA was purified from 50 µl of this chromatin sample using phenol/chloroform method and fragment size was checked through agarose gel electrophoresis (image not shown). For immunoprecipitation, 200 µl of chromatin sample was mixed with 25 µl of pre-washed HA beads (Sigma) and ChIP dilution buffer was added to make up the final volume to 300 µl. In Mock-IP A/G beads (Santa Cruz) were added at the place of HA beads. The mixed sample was kept for end-over-end rotation at 4°C for overnight. Beads were washed with low salt wash buffer (0.1% SDS, 1% TritonX-100, 2 mM EDTA, 20 mM Tris-HCl, pH 8, 150mM NaCl), high salt wash buffer (0.1% SDS, 1% TritonX-100, 2 mM EDTA, 20 mM Tris-HCl, pH 8, 0.5 M NaCl), LiCl wash buffer (25mM LiCl, 1% NP-40, 1% NaDOC, 1mM EDTA, 10mM Tris-Cl, pH 8), and TE buffer (10mM Tris-HCl, pH 8, 1mM EDTA). Beads were resuspended in 150 µl of ChIP elution buffer (50mM $NaHCO_3$, 1% SDS) and vortexed gently for 15 min at RT, followed by centrifuge at 2000 RPM for 4°C and supernatants were collected. This step was repeated two times and the samples were pooled and 1µl of RNase with 18µl of 5M NaCl was added and incubated at 67°C for 4-5 h. 25µl of 5X PK buffer (50mM Tris-HCl, pH 8, 25mM EDTA.$NA_2$, pH 8, 1.25 % SDS) and 1.5 µl proteinase K (10mg/ml) was added and incubated at 45°C for 2h. Thereafter, the DNA was purified using phenol/chloroform extraction and ethanol precipitation followed by resuspension in 30 µl of TE buffer. PCR was performed using the 2 µl of eluted DNA as template and following primers:

**Primers for promoter regions**

m3_Fw 5’-GATCCAATCCGAAAGCCG-3’

m3_Re 5’-CTAGTTCCCAGCCCTACT-3’

m5_Fw 5’-GTGGTTGTCTGTGTGGAG-3’

m5_Re 5’-GACCTGCTACCTGCGAACA-3’

m7_Fw 5’-GCACGCATGTTCCGTTTG-3’

m7_Re 5’-GGGAAACACTTTGCCCTC-3’

m8_Fw 5’-GCCAATATGCCACATCCAC-3’

m8_Re 5’-GGAACAGCTGCAACTTCG-3’

mβ_Fw 5’-ACTTCGATCGGTTCCCAG-3’

mβ_Re 5’-GAACTGGACAGTGAGTGC-3’

mδ_Fw 5’-GCGGCACAATCCCAATAC-3’

mδ_Re 5’-CTGGTTCCCACTTCCCT-3’

mγ_Fw 5’-CACTCCGTTTACAAATCCCTG-3’

mγ_Re 5’-GCTAGACCTTCGGTGATC-3’

## Acknowledgments

The authors are thankful to Spyros Artavanis-Tsakonas for Notch pathway mutant *Drosophila* stocks. Jessica Treisman and Sarah Bray are acknowledged for *Su(H)VP16* stocks and Jemeen Sreedharan is acknowledged for providing *htk* mutant alleles. The Bloomington stock centre is acknowledged for providing fly stocks. Fellowship support to A.S. and D.D. were provided by CSIR, and M.S.P by JNMF fellowship. We acknowledge the confocal facility of DBT-BHU-ISLS, B.H.U. This work was supported by grants from Department of Biotechnology, Government of India to A.M. and M.M. Authors declare no competing interests.

## References


1. **Akhtar, A., Zink, D. and Becker, P. B**. (2000). Chromodomains are protein-RNA interaction modules. *Nature*. **407**, 405-409.
2. **Andersson, E. R., Sandberg, R. and Lendahl, U.** (2011). Notch signaling: simplicity in design, versatility in function. *Development*. **138**, 3593–3612.
3. **Artavanis-Tsakonas, S., Rand, M. D. and Lake RJ.** (1999). Notch signaling: cell fate control and signal integration in development. *Science.* **284**, 770–776.
4. **Baron, M., Aslam, H., Flasza, M., Fostier, M., Higgs, J. E., Mazaleyrat, S. L. and Wilkin, M. B.** (2002). Multiple levels of Notch signal regulation. *Mol Membr Biol*. **19**, 27–38.
5. **Blaumueller, C. M., Qi, H., Zagouras, P. and Artavanis-Tsakonas, S.** (1997). Intracellular cleavage of Notch leads to a heterodimeric receptor on the plasma membrane. *Cell*. **90**, 281–291.
6. **Borggrefe, T. and Oswald, F.** (2016). Setting the Stage for Notch: The *Drosophila* Su(H)-Hairless Repressor Complex. *PLoS Biol*. **14**, 1-8.
7. **Bouazoune, K., Mitterweger, A., Langst, G., Imhof, A., Akhtar, A., Becker, P. B., and Brehm, A.** (2002). The dMi-2 chromodomains are DNA binding modules important for ATP-dependent nucleosome mobilization. *EMBO J.* **21**, 2430-2440.
8. **Brand, A. H. and Perrimon, N.** (1993). Targeted gene expression as a means of altering cell fates and generating dominant phenotypes. *Development.* **118**, 401–415.
9. **Bray, S. and Furriols, M.** (2001). Notch pathway: Making sense of Suppressor of Hairless. *Current Biology.* **11**, 217–221.
10. **Brehm, A., Langst, G., Kehle, J., Clapier, C. R., Imhof, A., Eberharter, A., Müller, J. and Becker, P. B.** (2000). dMi-2 and ISWI chromatin remodeling factors have distinct nucleosome binding and mobilization properties. *EMBO J.* **19**, 4332-4341.
11. **Brou, C., Logeat, F., Gupta, N., Bessia, C., LeBail, O., Doedens, J. R., Cumano, A., Roux, P., Black, R. A. and Israël, A.** (2000). A novel proteolytic cleavage involved in Notch signaling: the role of the disintegrin-metalloprotease TACE. *Mol. Cell.* **5**, 207–216.
12. **Cabrera, C. V.** (1990). Lateral inhibition and cell fate during neurogenesis in *Drosophila*: the interactions between scute, Notch and Delta. *Development.* **110**, 733-742.

13. **Cao, J., Gao, T., Stanbridge, E. J. and Irie, R.** (2001). RBP1L1, a retinoblastoma-binding protein-related gene encoding an antigenic epitope abundantly expressed in human carcinomas and normal testis. *J. Natl. Cancer Inst.* **93**, 1159–1165.
14. **Casso, D. J., Biehs, B. and Kornberg, T. B**. (2010). A Novel Interaction Between hedgehog and Notch Promotes Proliferation at the Anterior–Posterior Organizer of the *Drosophila* Wing. *Genetics.* **187**, 485–499.
15. **Cau, E. and Blader, P.** (2009). Notch activity in the nervous system: to switch or not switch? *Neural Development.* **4**, 1-11.
16. **de Celis, J. F., de Celis, J., Ligoxygakis, P., Preiss, A., Delidakis, C. and Bray, S.** (1996). Functional relationships between Notch, Su(H) and the bHLH genes of the E(spl) complex: the E(spl) genes mediate only a subset of Notch activities during imaginal development. *Development.* **122,** 2719–2728.
17. **De Strooper, B., Annaert ,W., Cupers, P., Saftig, P., Craessaerts, K., Mumm, J. S., Schroeter, E. H., Schrijvers, V., Wolfe, M. S., Ray, W. J., et al.** (1999). A presenilin-1-dependent gamma-secretase-like protease mediates release of Notch intracellular domain. *Nature*. **398**, 518–522.
18. **Defeo-Jones, D., Huang, P. S., Jones, R. E., Haskell, K. M., Vuocolo, G. A., Hanobik, M. G., Huber, H. E. and Oliff, A.** (1991). Cloning of cDNAs for cellular proteins that bind to the retinoblastoma gene product. *Nature*. **352**, 251-254.
19. **Delidakis, C. and Artavanis-Tsakonas, S**. (1992). The Enhancer of split [E(spl)] locus of *Drosophila* encodes seven independent helix-loop-helix proteins. *Proc. Natl. Acad. Sci. USA.* **89**, 8731–8735.
20. **Egan, S. E., St-Pierre, B. and Leow, C. C.** (1998). Notch receptors, partners and regulators: from conserved domains to powerful functions. *Curr Top Microbiol Immunol.* **228**, 273–324.
21. **Fehon, R. G., Johansen, K., Rebay, I. and Artavanis-Tsakonas, S.** (2007). Complex cellular and subcellular regulation of notch expression during embryonic and imaginal development of *Drosophila*: implications for notch function, *J. Cell Biol*. **113**, 657–669.
22. **Fleischer, T. C, Yun, U. J. and Ayer, D. E.** (2003). Identification and characterization of three new components of the mSin3A corepressor complex. *Mol. Cell. Biol.* **23**, 3456–3467.

23. **Fortini, M. E. and Artavanis-Tsakonas, S.** (1994). The Suppressor of Hairless protein participates in Notch receptor signaling. *Cell.* **79**, 273–282.
24. **Fortini, M. E.** (2009). Notch signaling: the core pathway and its posttranslational regulation. *Dev. Cell.* **16**, 633–647.
25. **Furiols, M. And Bray, S.** (2000). Dissecting the mechanisms of Suppressor of Hairless function. *Dev. Biol.* **227**, 520-532.
26. **Gaudet, P., Livstone, M. and Thomas, P.** (2010). Gene Ontology annotation inferences using phylogenetic trees. GO Reference Genome Project. http://www.geneontology.org/cgi-bin/references.cgi#GO_REF0000033.
27. **Giaimoa, B. D., Oswaldb, F. and Borggrefe, T.** (2017). Dynamic chromatin regulation of Notch target genes. *Transcription*. **8**, 61–66.
28. **Go, M. J. and Artavanis-Tsakonas, S.** (1998). A genetic screen for novel components of the Notch signaling pathway during *Drosophila* bristle development. *Genetics*. **150**, 211-220.
29. **Guruharsha, K. G., Kankel, M. W. and Artavanis-Tsakonas, S.** (2012). The Notch signalling system: recent insights into the complexity of a conserved pathway. *Nat. rev. Genet.* **13**, 654–666.
30. **Hartenstein, V., Posakony, J. W.** (1990). A dual function of the Notch gene in *Drosophila* sensillum development. *Dev. Biol.* **142**, 13–30.
31. **Helms, W., Lee, H., Ammerman, M., Parks, A. L., Muskavitch, M. A. and Yedvobnick, B.** (1999). Engineered truncations in the *Drosophila* mastermind protein disrupt Notch pathway function. *Dev. Biol.* **215**, 358–374.
32. **Herrscher, R. F., Kaplan, M. H., Lelsz, D. L., Das, C., Scheuermann, R. and Tucker, P. W.** (1995). The immunoglobulin heavy-chain matrix-associating regions are bound by Bright: a B cell-specific trans-activator that describes a new DNA-binding protein family. *Genes Dev.* **24**, 3067–82.
33. **Iwahara, J. and Clubb, R. T.** (1999). Solution structure of the DNA binding domain from Dead ringer, a sequence-specific AT-rich interaction domain (ARID). *The EMBO J.* **21**, 6084-6094.

34. **Iwahara, J., Iwahara, M., Daughdrill, G. W., Ford, J. and Clubb, R. T.** (2002). The structure of the Dead ringer-DNA complex reveals how AT-rich interaction domains (ARIDs) recognize DNA. *The EMBO J.* **5**, 1197-1209.
35. **Kadosh, D. and Struhl, K.** (1998). Histone deacetylase activity of Rpd3 is important for transcriptional repression in vivo. *Genes Dev.* **12**, 797–805.
36. **Kankel, M. W., Hurlbut, G. D., Upadhyay, G., Yajnik, V., Yedvobnick, B. and Artavanis-Tsakonas, S.** (2007). Investigating the Genetic Circuitry of Mastermind in *Drosophila*, a Notch Signal Effector. *Genetics*. **177**, 2493–2505.
37. **Kim, J., Daniel, J., Espejo, A., Lake, A., Krishna, M., Xia, L., Zhang, Y., Bedford, M. T**. (2006). Tudor, MBT and chromo domains gauge the degree of lysine methylation. *EMBO Rep.* **7**, 397–403.
38. **Lai, A., Marcellus, R. C., Corbeil, H. B. and Branton, P. E.** (1999). RBP1 induces growth arrest by repression of E2F-dependent transcription. *Oncogene.* **18**, 2091–2100.
39. **Lai, A., Kennedy, B. K., Barbie, D. A., Bertos, N. R., Yang, X. J., Theberge, M. C., Tsai, S. C., Seto, E., Zhang, Y., Kuzmichev, A., et al.** (2001). RBP1 recruits the mSIN3-histone deacetylase complex to the pocket of retinoblastoma tumor suppressor family proteins found in limited discrete regions of the nucleus at growth arrest. *Mol. Cell. Biol.* **21**, 2918–2932.
40. **Lai, A., Kennedy, B. K., Barbie, D. A., Bertos, N. R., Yang, X. J., Theberge, M.-C., Tsai, S.-C., Seto, E., Zhang, Y., Kuzmichev, A., Lane, W. S., Reinberg, D., Harlow, E. and Branton, P. E.** (2001). RBP1 recruits the mSIN3-histone deacetylase complex to the pocket of retinoblastoma tumor suppressor family proteins found in limited discrete regions of the nucleus at growth arrest. *Molec. Cell. Biol.* **21**, 2918-2932.
41. **Lee T. and Luo L.** (2001). Mosaic analysis with a repressible cell marker (MARCM) for Drosophila neural development. *Trends Neurosci*. **24**, 251–254.
42. **Liu, J., Sato, C., Cerletti, M. and Wagers, A.** (2010). Notch signaling in the regulation of stem cell self-renewal and differentiation. *Curr. Top Dev. Biol.* **92**, 367–409.
43. **Logeat, F., Bessi, C., Brou, C., Lebail, O., Jarriault, S., Seidahng, N. G. and Israel, A.** (1998). The Notch1 receptor is cleaved constitutively by a furin-like convertases. *Proc. Natl. Acad. Sci. USA*. **95**, 8108-8112.

44. **Mukherjee, A., Veraksa, A., Bauer, A., Rosse, C., Camonis, J. and Artavanis-Tsakonas, S.** (2005). Regulation of Notch signalling by non-visual β-arrestin. *Nat. Cell Biol.* **7**, 1191–1201.
45. **Mumm, J. S., Schroeter, E. H., Saxena, M. T., Griesemer, A., Tian, X., Pan, D. J., Ray W. J. and Kopan, R.** (2000). A ligand-induced extracellular cleavage regulates gamma-secretase-like proteolytic activation of Notch1. *Mol Cell*. **5**, 197–206.
46. **Neumann, C. J. and Cohen, S. M.** (1996). A hierarchy of cross-regulation involving Notch, wingless, vestigial and cut organizes the dorsal/ventral axis of the *Drosophila* wing. *Development.* **122**, 3477–3485.
47. **Patsialou, A., Wilsker, D. and Moran, E.** (2005). DNA-binding properties of ARID family proteins. *Nucleic Acids Research*. **33**, 66-80.
48. **Rebay, I., Fleming, R. J., Fehon, R. G., Cherbas, L., Cherbas, P. and Artavanis-Tsakonas, S.** (1991). Specific EGF repeats of Notch mediate interactions with Delta and Serrate: implications for Notch as a multifunctional receptor. *Cell*. **67**, 687–699.
49. **Sachan, N., Mishra, A. K., Mutsuddi, M. and Mukherjee, A.** (2013). The *Drosophila* importin-α3 is required for nuclear import of Notch in vivo and it displays synergistic effects with Notch receptor on cell proliferatio. *PLoS One.* **8**, 2-10.
50. **Silverstein, R. A. and Ekwall, K.** (2005) Sin3: a flexible regulator of global gene expression and genome stability. *Curr. Genet*. **47**, 1–17.
51. **Singh, A., Dutta, D., Paul, M. S., Verma, D., Mutsuddi, M. and Mukherjee, A.** (2018). Pleiotropic Functions of the Chromodomain-Containing Protein Hat-trick During Oogenesis in *Drosophila melanogaster*. *G3- Genes Genom Genet*. **8**, 1067-1077.
52. **Spain, M. M., Caruso, J. A., Swaminathan, A. and Pile, L. A.** (2010). *Drosophila* SIN3 Isoforms interact with distinct proteins and have unique biological functions. *The Journal of Biochemistry.* **285**, 27457-27467.
53. **Sreedharan, J., Neukomm, L. J., Brown, R. H. and Freeman, M. R.** (2015). Age-Dependent TDP-43-Mediated Motor Neuron Degeneration Requires GSK3, hat-trick, and xmas-2. *Curr. Biol.* **25**, 2130-2136.
54. **Struhl, G. and Adachi, A.** (1998). Nuclear access and action of Notch in vivo. *Cell.* **93**, 649–660.

55. **Struhl, G. and Greenwald, I.** (1999). Presenilin is required for activity and nuclear access of Notch in *Drosophila*. *Nature*. **398,** 522–525.
56. **Suryadinata, R., Sadowski, M., Steel, R. and Sarcevic, B.** (2011). Cyclin-dependent kinase-mediated phosphorylation of RBP1 and pRb promotes their dissociation to mediate release of the SAP30.mSin3.HDAC transcriptional repressor complex. *J. Biol. Chem*. **286**, 5108–5118.
57. **Wan, C., Borgeson, B., Phanse, S., Tu, F., Drew, K., Clark, G., Xiong, X., Kagan, O., Kwan, J., Bezginov, A. et al.** (2015). Panorama of ancient metazoan macromolecular complexes. *Nature*. **17**, 339-44.
58. **Wang, Z., Lyu, J., Fang W., Miao, C., Nan, Z., Zhang, J., Xi, Y., Zhou, Q., Yang, X. and Ge1, W.** (2018). The histone deacetylase HDAC1 positively regulates Notch signaling during *Drosophila* wing development. *Biol Open*. **15**, 1-8.
59. **Wu, L., Aster, J. C., Blacklow, S. C., Lake, R., Artavanis-Tsakonas, S. and Griffin, J. D.** (2000). MAML1, a human homologue of *Drosophila* mastermind, is a transcriptional co-activator for NOTCH receptors. *Nat. Genet.* **26**, 484–489.
60. **Xu, T. and Rubin, G. M.** (1993). Analysis of genetic mosaics in developing and adult *Drosophila* tissues. *Development*. **117**, 1223–1237.
61. **Ye, Y., Lukinova, N. and Fortini, M. E**. (1999). Neurogenic phenotypes and altered Notch processing in *Drosophila* Presenilin mutants. *Nature*. **398,** 525–529.
62. **Zhan, L., Hanson, K. A., Kim, S. H., Tare, T., Tibbetts, R. S.** (2013). Identification of Genetic Modifiers of TDP-43 Neurotoxicity in *Drosophila*. *PLoS One*. **8**, 1-14.
63. **Zhou, S., Fujimuro, M., Hsieh, J. J., Chen, L., Miyamoto, A., Weinmaster, G. and Hayward, S. D.** (2000). SKIP, a CBF1-associated protein, interacts with the ankyrin repeat domain of NotchIC to facilitate NotchIC function. *Mol. Cell. Biol*. **20**, 2400-2410.

## Figures

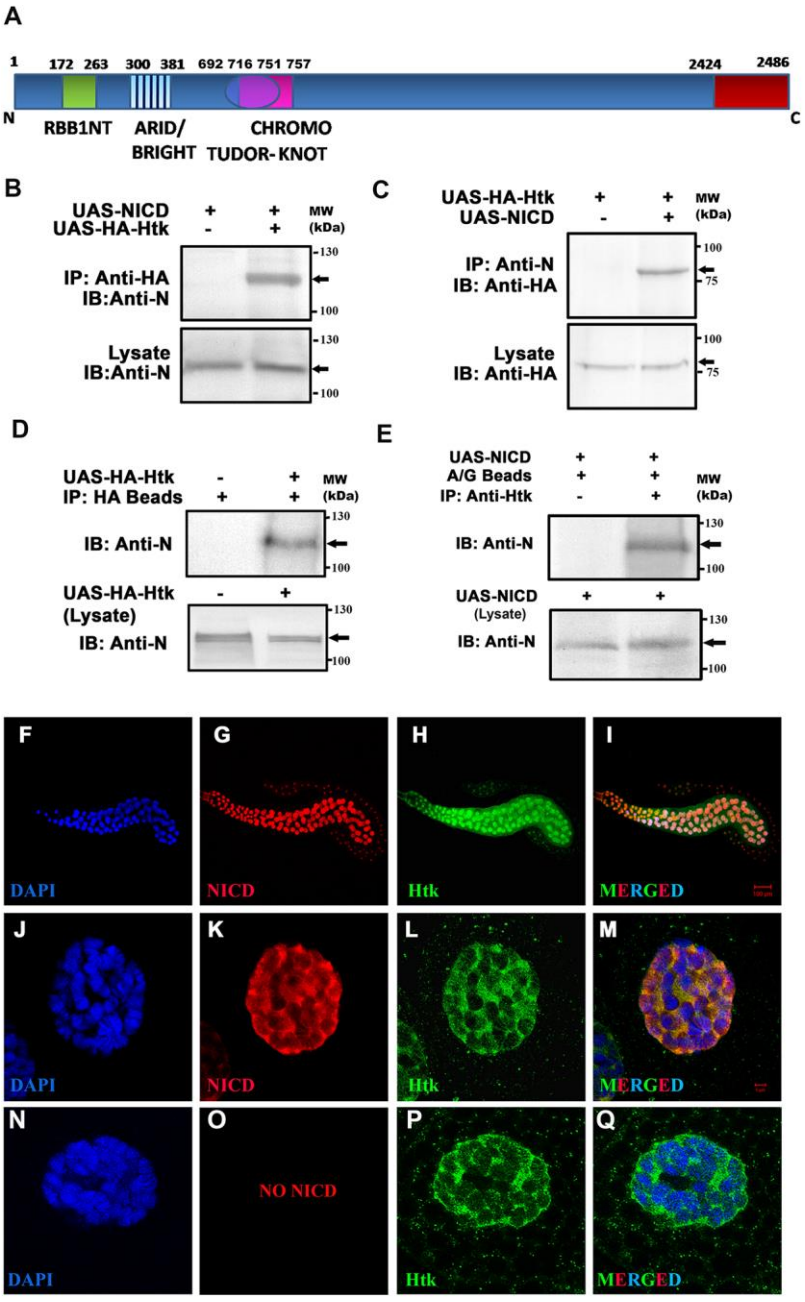


**Figure 1: *Drosophila* Notch binds with Htk. (A)** Schematic representation of Htk protein and its conserved domains. A specific region of Htk at C-terminal end (amino acids 2424–2486) was used for antibody generation. RBBNT- Retinoblastoma Binding Protein 1 N-terminal domain, ARID-AT Rich Interacting Domain, CHROMO-Chromatin Organization

Modifier **(B-C)** Co-immunoprecipitation was carried out with wing disc lysate over-expressing HA-Htk and Notch-ICD using *vg-GAL4*. (+) Symbol indicates the presence and (–) symbol shows the absence of specified reagent. **(B)** HA-Htk immunoprecipitated Notch-ICD that was detected by anti-Notch antibody (C17.9C6). **(C)** Notch-ICD also immunoprecipitated HA-Htk that was detected by anti-HA antibody. **(D)** Protein lysate was made from tissue over-expressing HA-Htk alone, and from wild-type tissue (only endogenous Htk), and HA-Htk was able to co-immunoprecipitate endogenous Notch. No Notch protein bands were observed in negative control. **(E)** Co-immunoprecipitation was carried out using anti-Htk antibody with larval salivary gland lysate in which Notch-ICD was over-expressed by *sgs-GAL4*. Endogenous Htk was sufficient to immunoprecipitate expressed Notch-ICD that was detected by anti-Notch antibody**.** Lower blot in each experiment shows the presence of specified protein in both the experimental and control lysates. (**F-M) Htk co-localized with expressed Notch in the cell nucleus.** Notch-ICD was expressed under the control of *sgs-GAL4* and was stained with anti-Notch antibody **(**Red**; G, K).** DAPI marks the chromatin (Blue; **F, J, N**). Anti-Htk antibody was used to stain endogenous Htk protein **(**Green**; H, L, P).** Second row is higher magnification image of a single cell of salivary gland from first row**. (I, M)** Merged images show that Htk and Notch co-localized in the cell nucleus **(I),** within chromatin and inter-chromatin spaces **(M). (N-Q)** Third row is the higher magnification image of single cell of larval salivary gland showing the expression of endogenous Htk without Notch-ICD over-expression. Notch-ICD over-expression does not cause any significant change in the expression and localization of endogenous Htk (L, P). Images in I, M and Q are merges of those in F-H, J-L and N-P, respectively. Scale bars, 100 μM (F-I) and 5 μM (J-Q).

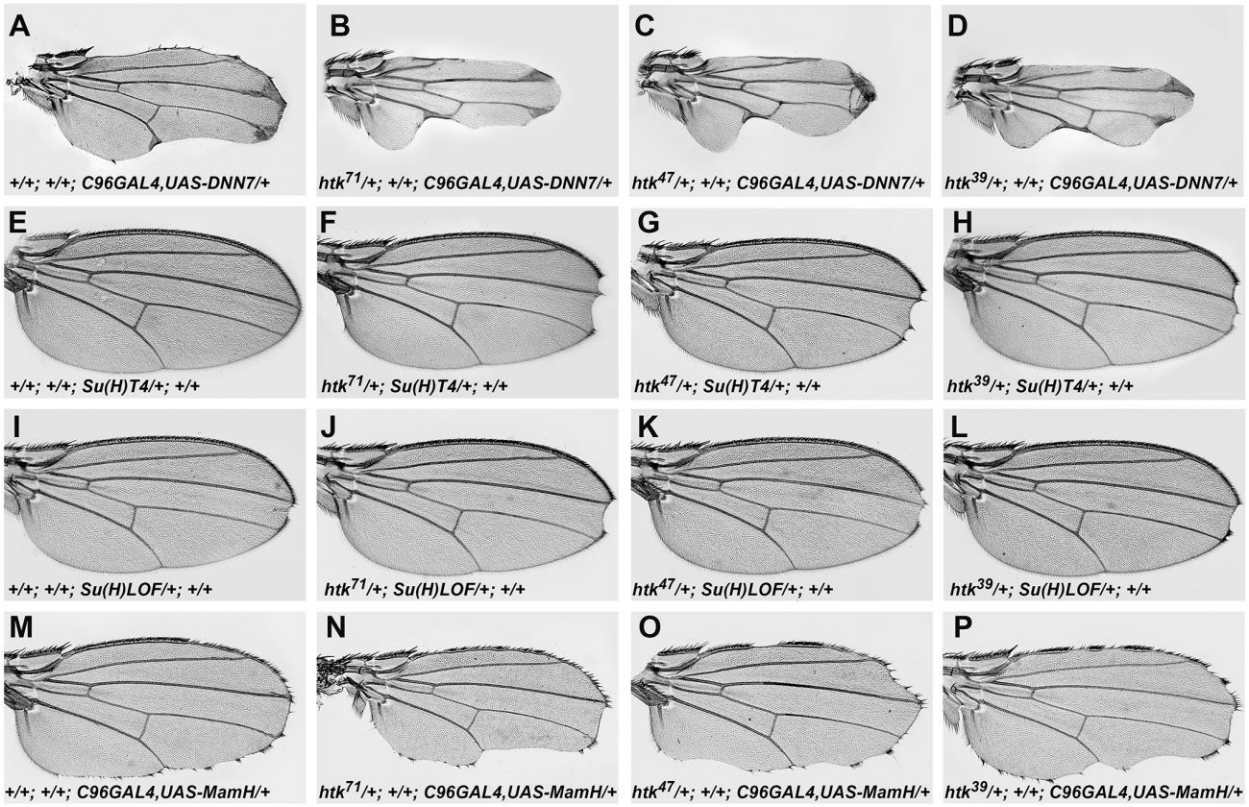


**Figure 2: Genetic interactions of *htk* with Notch pathway components.** Representative wings from different Notch pathway component mutants are shown in first column and in trans-heterozygous combination with *htk* mutants $htk^{71}$, $htk^{47}$, and $htk^{39}$ are shown in column second, third and fourth, respectively. **(A-D)** Dominant-negative Notch driven at wing margin using *C96-GAL4* caused wing notching phenotype (A) which was enhanced in trans-heterozygous combination with different *htk* alleles and the wings appeared shorter (B-D). **(E-L)** Similarly, when Su(H) gain-of-function allele**,** *Su(H)T4* (E) and loss-of-function allele, *Su(H)1* (I) were brought with different *htk* alleles, wing nicking phenotypes were increased. **(M-P)** Serration phenotype of wing expressing dominant-negative *mastermind* using *C96-GAL4* (M) was enhanced in combination with *htk* alleles. n=100 wings for each genotype. The penetrance of the phenotype for each genotype were 100% except for *Su(H)T4* heterozygotes with *htk* alleles in which penetrance of the phenotype was 85%.

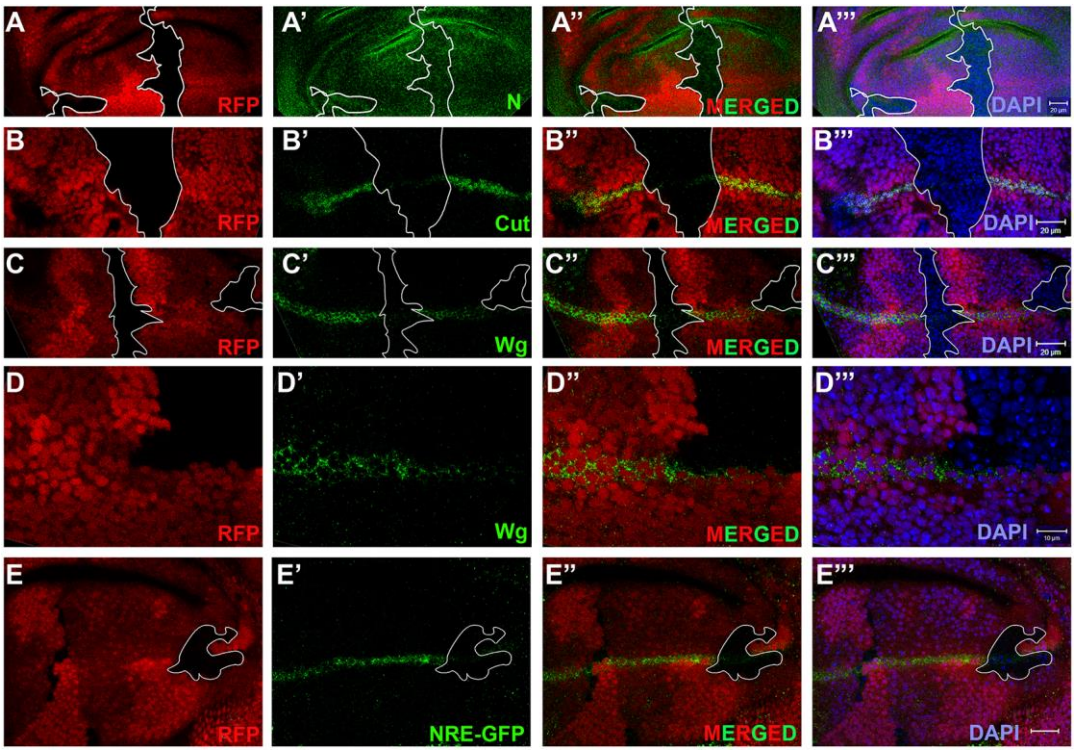


**Figure 3: Loss-of-function clones of *htk* displayed reduced Notch signaling activity without significantly affecting its endogenous localization and expression. (A–E''')** Loss-of-function clones of *htk* using $htk^{71}$ allele were generated with FLP/FRT system and $htk^{71}$ clones were marked by absence of RFP expression. **(A-C''', E-E''')** is lower magnification, **D-D'''** are higher magnification images. Notch staining in wing discs of such clones displayed no significant change in localization and expression of endogenous Notch **(A'),** while Notch downstream targets expression, Cut **(B')** and Wingless **(C', D')**, and the expression of a Notch signaling reporter line, NRE-GFP **(E'),** were significantly reduced in *htk* loss-of-function clones. Third column images are merges of those in first and second column. Fourth column shows merge images with DAPI staining in discs that showed integrity of nuclei. Scale bars: **(A–C''', E-E''')** 20 μM, **(D–D''')** 10 μM.

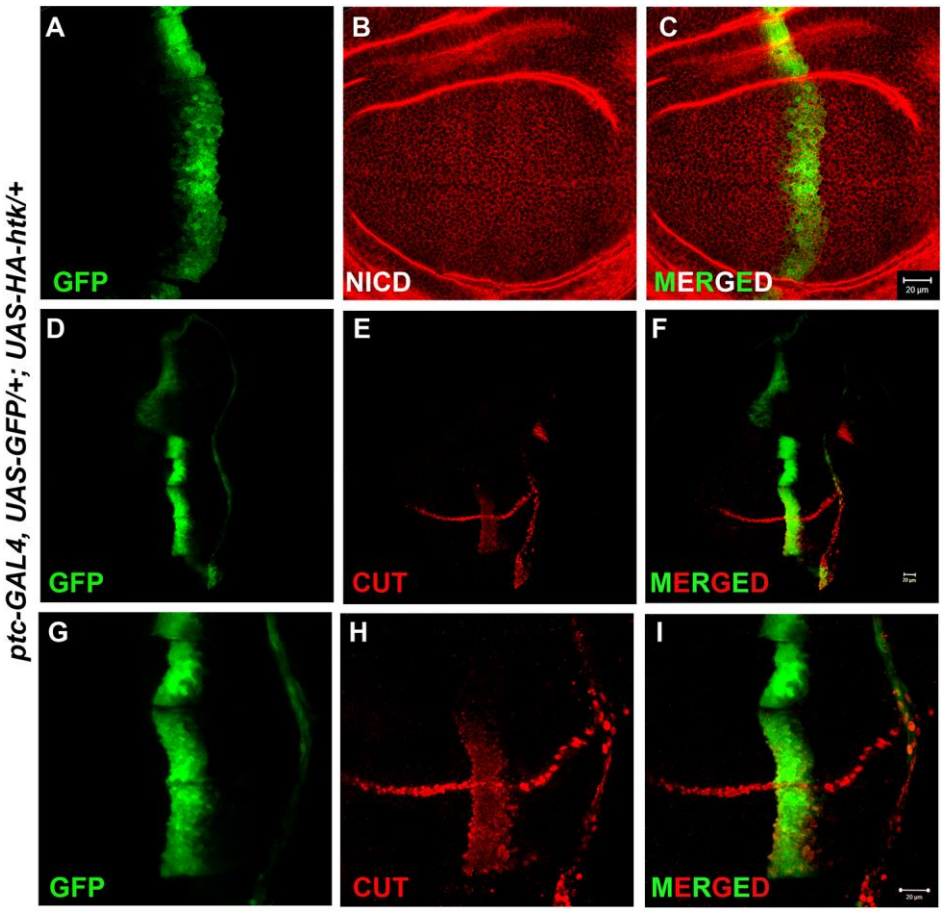


**Figure 4: Effect of over-expression of *htk* on Notch expression and its signaling activity at the dorso-ventral boundary of the wing disc. (A-C)** *patched-GAL4* driven expression of HA-Htk at the anterior/posterior boundary of the wing disc (marked with GFP) (first column), results in no change in Notch (red) expression. **(D-F)** Ectopic expression of Notch target, Cut at the anterior-posterior boundary is clearly visible in the pouch region of wing disc. **(G-I)** Higher magnification images of D-F, respectively. Scale bar, 20 μm.

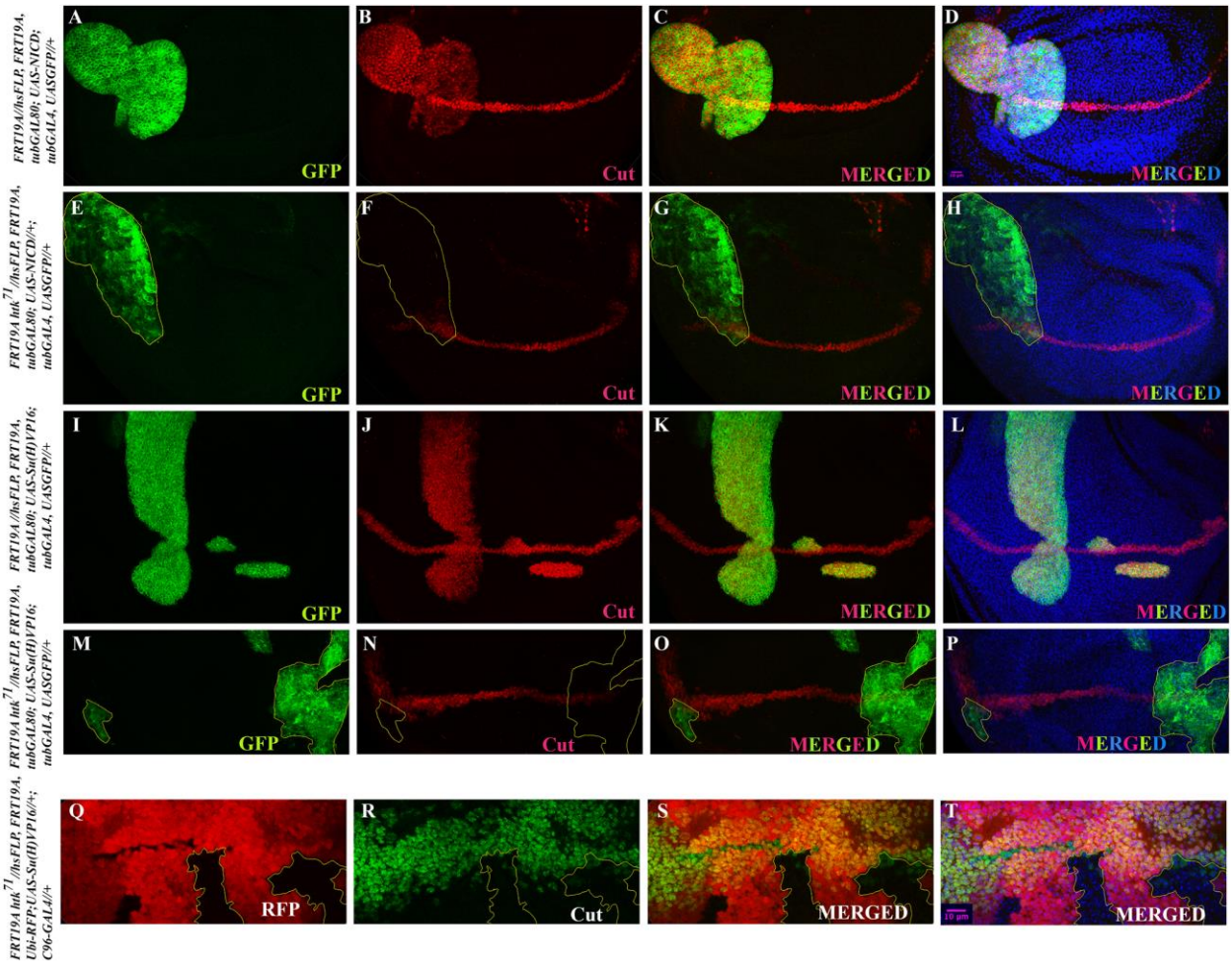


**Figure 5**: ***htk* is required for complete Notch signaling activity. (A-P)** MARCM analysis to show epistatic interaction of *htk* with *Notch* and *Su(H).* GFP marked MARCM-derived clones were generated in wing imaginal discs. Images in first column represents the clonal area, and second column shows expression of Notch downstream target, Cut. Images in third and fourth column are merged images of first and second column, and along with DAPI, respectively. Cut expression was checked in MARCM-derived *NICD* **(E-H)** or *Su(H)VP16* **(M-P)** over-expressing $htk^{71}$mutant clones and wild-type **(A-D, I-L)** clones**. (Q-T)** *Su(H)VP16* was over-expressed using *C96-GAL4* at dorso-ventral boundary, and in this background *htk* mutant FLP-FRT clones (marked as RFP null) were generated. Ectopic expression of Cut caused by over-expression of *NICD* and *Su(H)VP16* was significantly reduced in absence of *htk* which confirmed that NICD and Su(H) could not achieve its full activity in absence of Htk. Scale bar, 10µm.

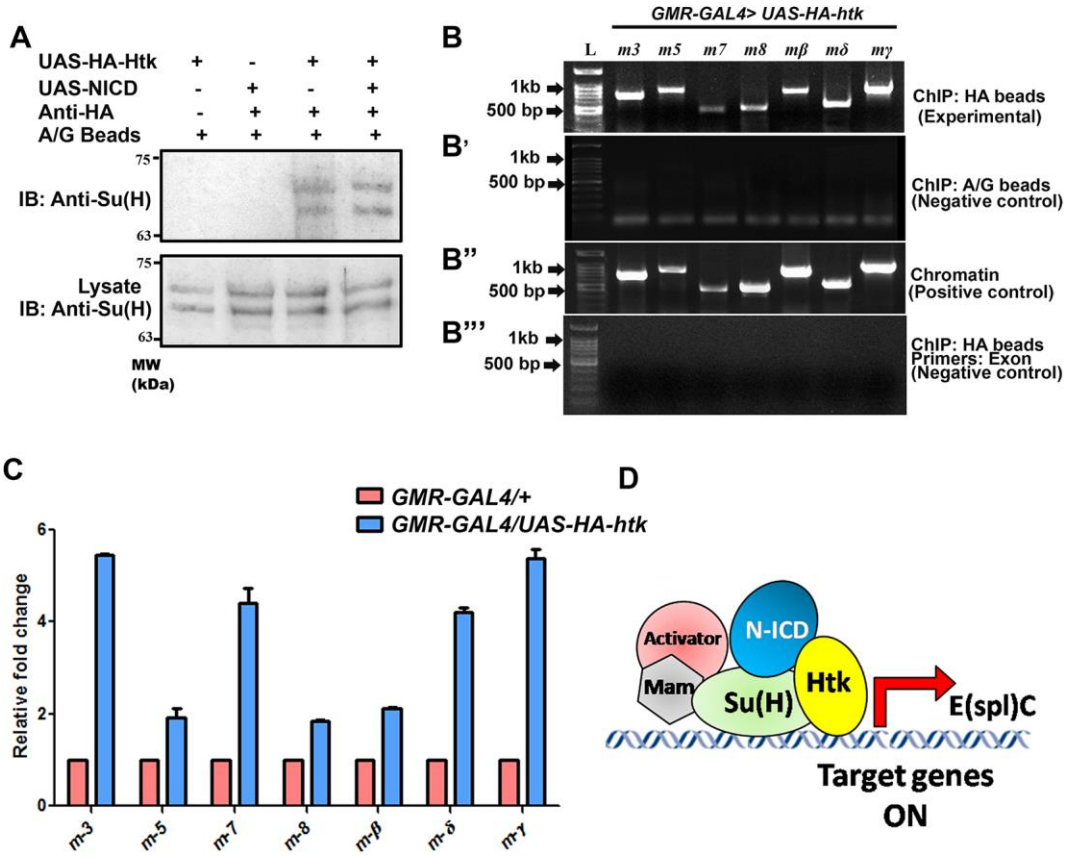


**Figure 6: Htk is a component of Notch-activation complex. (A)** Co-immunoprecipitation experiment using lysate prepared from wing disc over-expressing only Notch-ICD, only HA-Htk, and Notch-ICD along with HA-Htk using *vg-GAL4* driver line. Co-immunoprecipitation using lysate over-expressing Notch-ICD and HA-Htk revealed that Htk can co-immunoprecipitate endogenous Su(H). Additionally, Htk is sufficient to immunoprecipitate endogenous Su(H) when only endogenous Notch was present. Lower blot shows the presence of Su(H) in both the experimental and control lysates. Symbol (+) indicates the presence and symbol (–) shows the absence of specified reagent. **(B)** Chromatin immunoprecipitation experiment (ChIP) using chromatin prepared from adult head over-expressing HA-Htk driven with *GMR-GAL4*. Immunoprecipitation using HA-beads followed by PCR using purified immunoprecipitated DNA as templates and primers specific for regulatory sequences of Notch direct targets, *E(spl)* complex genes, showed amplification confirming that Htk protein binds to the promoter sequences

of the *E(spl)* complex genes. No amplification was observed in negative control in which template DNA used was purified from No-IP chromatin samples (only A/G beads were added). Chromatin samples before immunoprecipitation contain all the genomic DNA fragments, and were used for positive control. No amplification was observed in PCR from purified immunoprecipitated DNA using primers specific for exon sequences of *E(spl)* complex genes confirming that Htk could specifically bind and immunoprecipitate promoter sequences of *E(spl)c* genes. **(C)** Real-time PCR experiment using cDNA from adult head having endogenous htk, and over-expressed *htk* driven by GMR-GAL4 demonstrated a significant up-regulation of *E(spl)* complex genes when *htk* was over-expressed. Experiment was performed in triplicates. Error bars indicate standard error of the mean. (D) A concluding model depicting Htk as a component of Notch-Su(H) transcription activation complex.

A

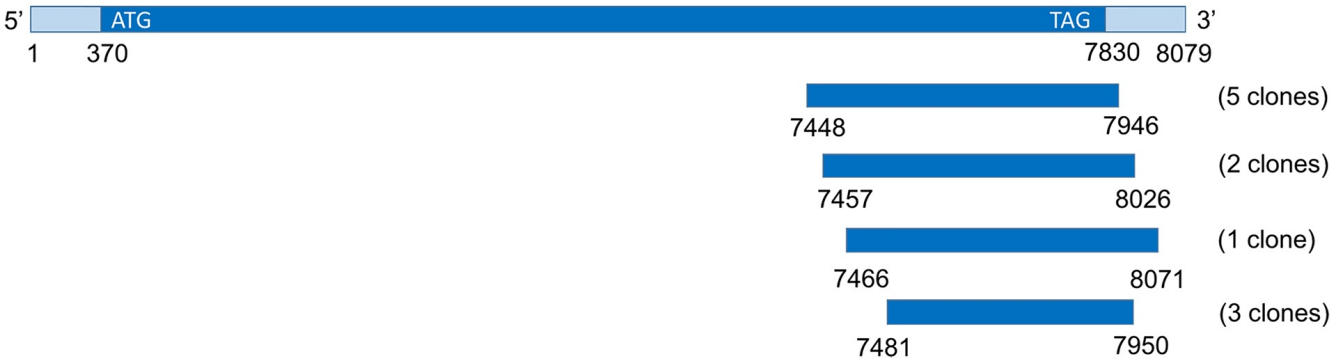


B

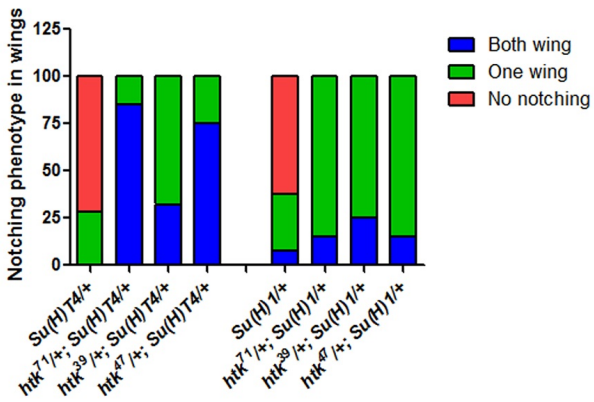


C

| Genotype | Phenotypes (%) |
|---|---|
| *+/+; ap-GAL4/+; UAS-htk-RNAi/+* | Extra vein material near 2nd Cross Vein : 46%<br>Defect in 2nd cross vein : 60%<br>Extra row of bristles near wing margin : 34%<br>1st vein defective : 100%<br>Patch of disorganized tissue at the tip of the vein : 60%<br>Blisters in wing : 14%<br>wings directed outward and upward : 100%<br>Increased scutellar bristles : 72% |
| *+/+; MS1096 –GAL4/+; UAS-htk-RNAi/+* | Extra row of bristles near wing margin : 89%<br>Patch of disorganized tissue at the tip of the vein : 72%<br>Defect in 1st cross vein : 52% |
| *+/+; +/+; C96 -GAL4 /UAS-htk-RNAi* | Defect in 1st cross vein : 44%<br>Extra vein : 12%<br>Unusual bristle pattern : 39%<br>Patch of disorganized tissue at the tip of the vein : 39% |
| *+/+; ptc-GAL4 /+;UAS-htk-RNAi/+* | Defect in 1st cross vein : 75%<br>Patch of disorganized tissue at the tip of the vein : 52.5%<br>Extra vein material near cross vein : 13%<br>1st cross vein very short and reduced intervein distance between L3-L4 : 100% |
| *+/+; +/+; dpp-Gal4/UAS-htk-RNAi* | Extra vein material near 2nd cross vein : 7.14%<br>Patch of disorganized tissue at the tip of the vein : 49%<br>Double 1st cross vein : 4% |
| *+/+; en-GAL4/+; UAS-htk-RNAi* | mis-oriented bristles and thinner wing blade in posterior region of wings : 75% |
| *+/+; ey-GAL4/+; UAS-htk-RNAi* | Reduced eye size :100% |

D

| Genotype | Phenotypes (100%) |
|---|---|
| *+/+; ap-GAL4/+; UAS-HA-htk/+* | • loss of scutellar bristles<br>• reduced size of scutellum<br>• severe wing blisters |
| *+/+; en-GAL4 /+; UAS-HA-htk/+* | • bending of third wing vein<br>• thinner wing blade<br>• incomplete fifth vein |
| *+/+; ey-GAL4 /+;UAS-HA-htk/+* | • loss of ommatidia |
| *+/+; +/+; GMR-Gal4/UAS-HA-htk* | • eye roughening |

**Figure S1: (A)** Schematic representation of the sequence range of 11 positive yeast two-hybrid clones which overlapped with *htk* cDNA, when amino terminus of Notch-ICD (amino acids 1765–1895) was used as bait to screen 6x10$^6$ cDNAs from a *Drosophila* 0–24 h embryonic library. **(B)** Graph showing the frequency (number) of wing notching phenotypes observed in *Su(H)T4* and *Su(H)1* alleles individually and in trans-heterozygous combination with different *htk* alleles: *htk$^{71}$, htk$^{39}$, htk$^{47}$*. **(C)** Development defects induced by down-regulation of *htk* with a variety of GAL4 drivers, n=200. **(D)** Defects observed in wing and eye when ectopic expression of HA-*htk* was induced with a variety of GAL4 drivers, n=200. All phenotypes examined were 100% penetrant.

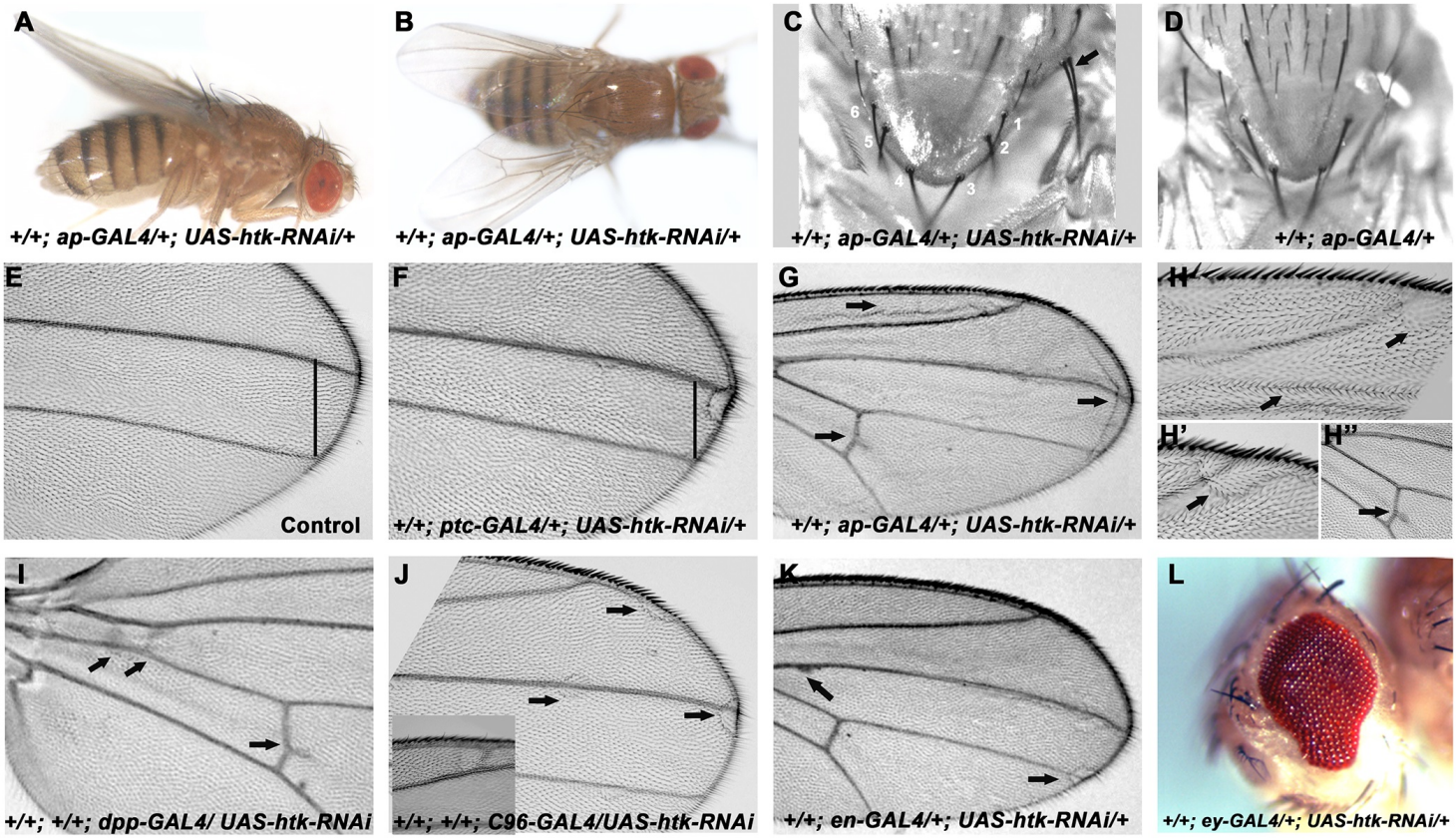


**Figure S2**: **Down-regulation of *htk* exhibits distinct phenotypes in *Drosophila* wings and eyes. (A-D, G)** *apterous-GAL4* driven *htk-RNAi* displayed upward (A) and outward (B) directed wings with extra rows of sensory bristles and vein material (arrow) in the wingblade (G), and increased scutellar bristles (C) compared to control (D). Similarly when *htk* was down-regulated at anterior-posterior boundary using *patched-GAL4* **(F)** and *dpp-GAL4* **(I),** at wing margin using using *C96-GAL4* **(J)**, in posterior compartment of wing using *engrailed-GAL4* **(K)**, and in the eye using *eyeless-GAL4* **(L)**, it resulted in reduced distance between L3 and L4 veins (black line) **(F)**, extra vein material (arrows) **(I)**, areas with thinner cuticle (arrows) **(J, K)** and reduced eye-size **(L)**, respectively. **(E)** Control adult wing displaying normal wing margin and longitudinal veins L1–L5. **(H-H")** High magnification images of wing showing extra row of bristles (H), area with thinner cuticle (H'), and extra vein material (H''). Several htk down-regulation phenotypes mimic Notch loss-of-function phenotypes.

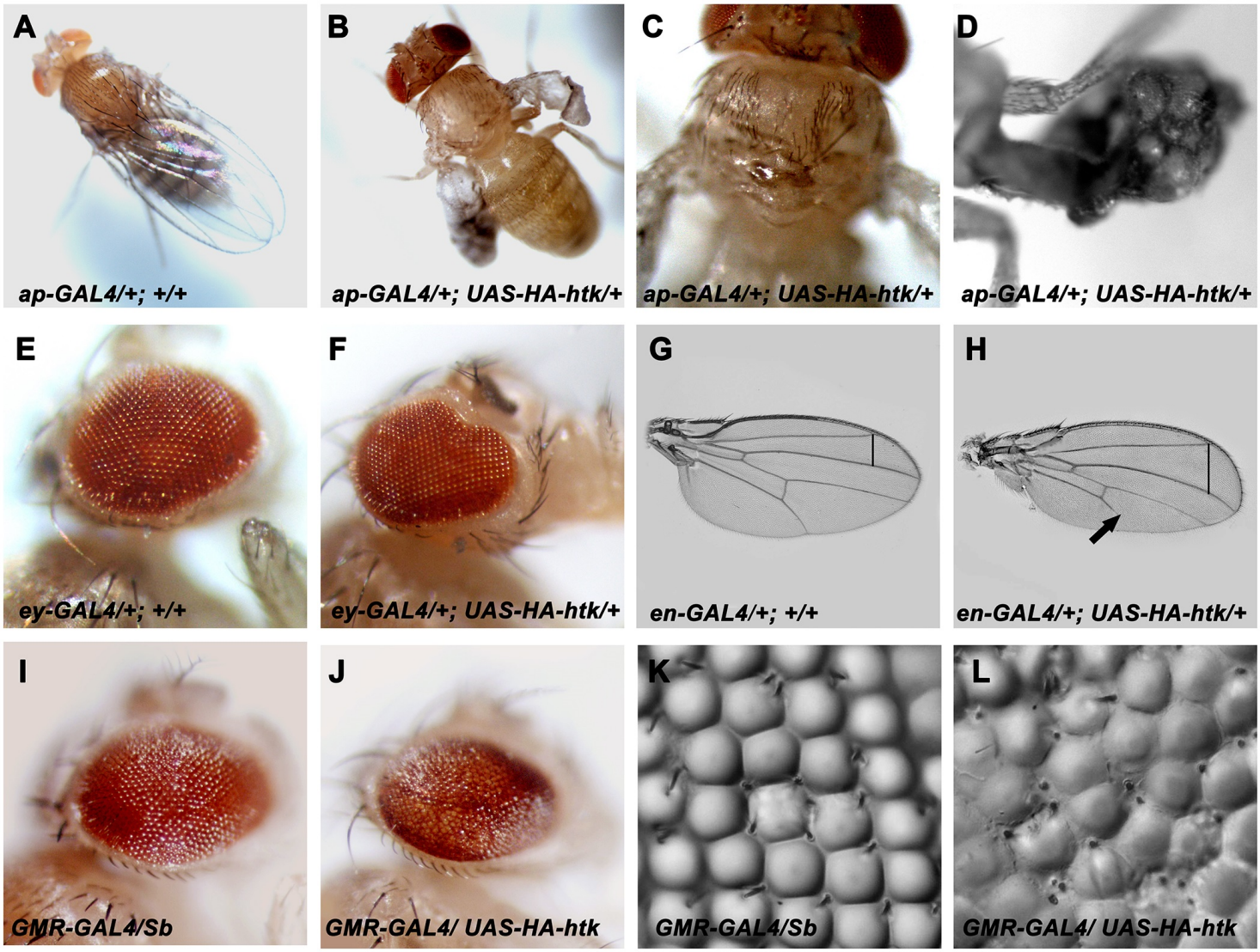


**Figure S3**: **Over-expression of *htk* resembles *Notch* gain-of-function phenotypes. (A-D)** Ectopic expression of *htk* driven by *apterous-GAL4* causes loss of scutellar bristles **(B, C)** and deformed wing **(B, D)** in comparison to only *apterous-Gal4/+* fly **(A)**. **(E,F)** *eyeless-GAL4* driven expression of *htk* in eye results in loss of ommatidia. **(G,H)** Over-expression of htk in posterior region of wing using *engrailed-GAL4* results in incomplete fifth vein and increased inter-vein distance between second and third vein. **(I, J)** Ectopic expression in adult eye using *GMR-GAL4* results in increased eye-roughening and loss of ommatidial bristles. **(K, L)** Nail polish imprint images of adult eye showing these eye phenotypes more clearly. Phenotypes showed 100% penetrance.

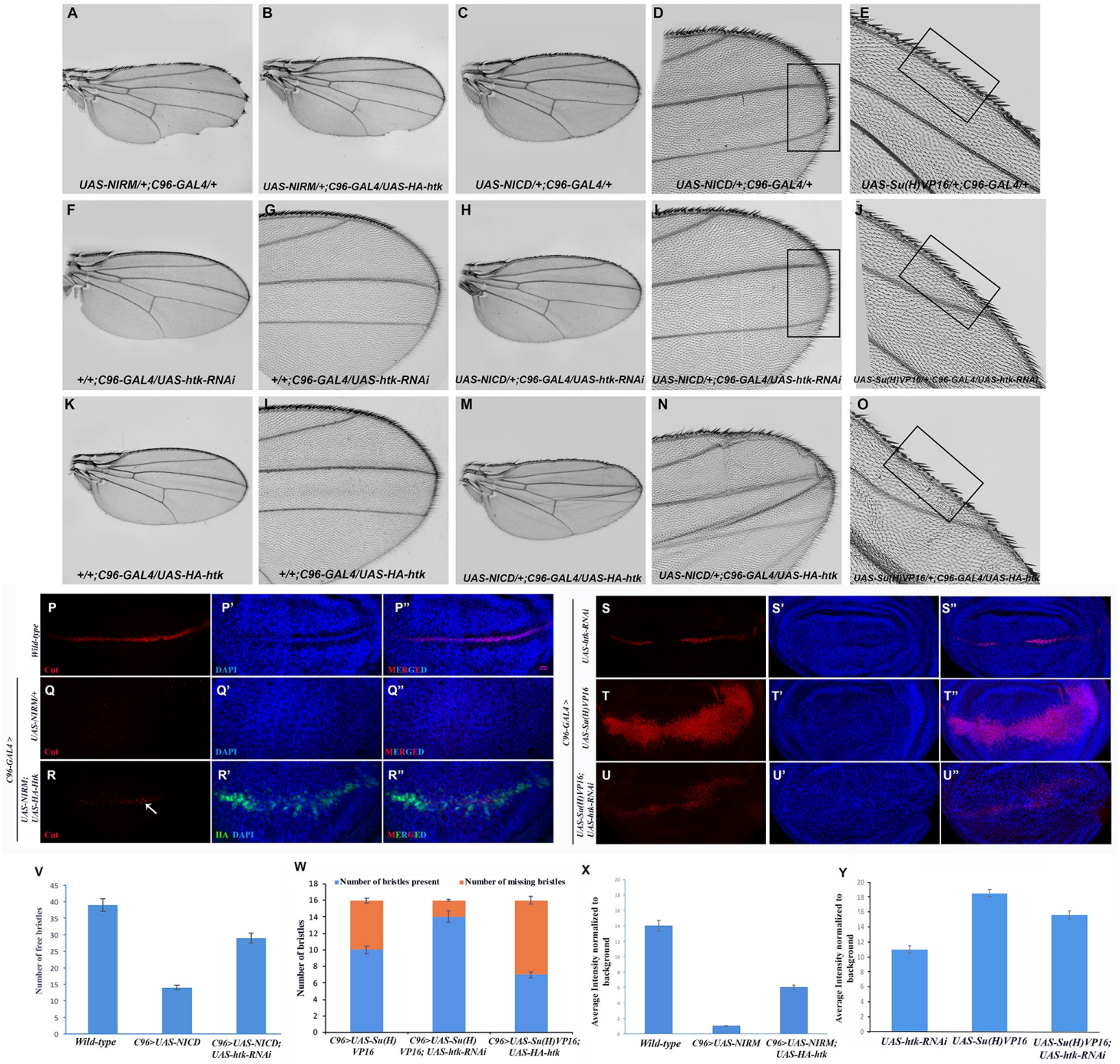


**Figure S4: Epistatic interactions of *htk* with Notch pathway.** *C96-GAL4* was used to drive the expression of different *UAS* lines at wing margin. **(A-O) Wing images showing epistatic and synergistic interactions between *htk* and *Notch* or *Su(H)VP16***. No notching or bristle irregularities were observed when *htk* was downregulated (F, G), or upregulated (K, L) at the wing margin. When the dose of *htk* was increased in *Notch* loss-of-function background, the wing notching phenotype caused by *Notch-RNAi* (A) was significantly rescued (B). Over-expression of *Notch* (C, D) and *Su(H)VP16* (E) at the wing margin resulted irregularities in wing bristle. This irregularity in bristle pattern was rescued when dosage of *htk* was reduced in this background (H-J). The irregularity in bristle localization was quantified by counting the number of free bristles in the same selected area of wing (n=10) expressing *Notch-ICD* alone and *Notch-ICD* along with *htk-RNAi* (boxed regions, 350µm length) **(V)**, and by counting the number of thick dorsal bristles present or absent in the same selected area of wing expressing *Su(H)VP16* alone and *Su(H)VP16* along with *htk-RNAi* (boxed region, 200µm length) **(W) [**error bars indicate standard error of the mean (n=3)]. The quantification is represented as the graph. Additionally, when *htk* along with *Notch* or *Su(H)VP16* were co-expressed, an increase in the wing margin irregularities was observed (M-O). All the phenotypes showed 100% penetrance (n=100). **(P-U'') Activity of Notch signaling was observed during epistatic interaction of *htk* with *Notch* and *Su(H)VP16***. Notch downstream marker, Cut was used to report the Notch signaling activity. DAPI marked the nuclei. The wild type Cut expression (P) was lost when Notch was reduced at dorso-ventral boundary of wing disc (Q). A rescue in the Cut expression was observed when *HA-htk* was over-expressed in the same background (R). (S-U'') Alternatively, ectopic expression of Cut caused by over-expression of *Su(H)VP16* (T) was partially rescued when *htk* was reduced in this background (U). Images in third column in both the panel are merged of images from first and second column. **(X, Y)** Quantification of Cut signal intensity at dorso-ventral boundary of wing disc is represented in the form of a graph. Cut signals are normalized to background signals, and values relative to controls are presented. Error bars indicate standard error of the mean (n=3). Figure D, G, I, L, N are higher magnification images of C, F, H, K, M, respectively. Scale bar, (P-U'') 10µm.

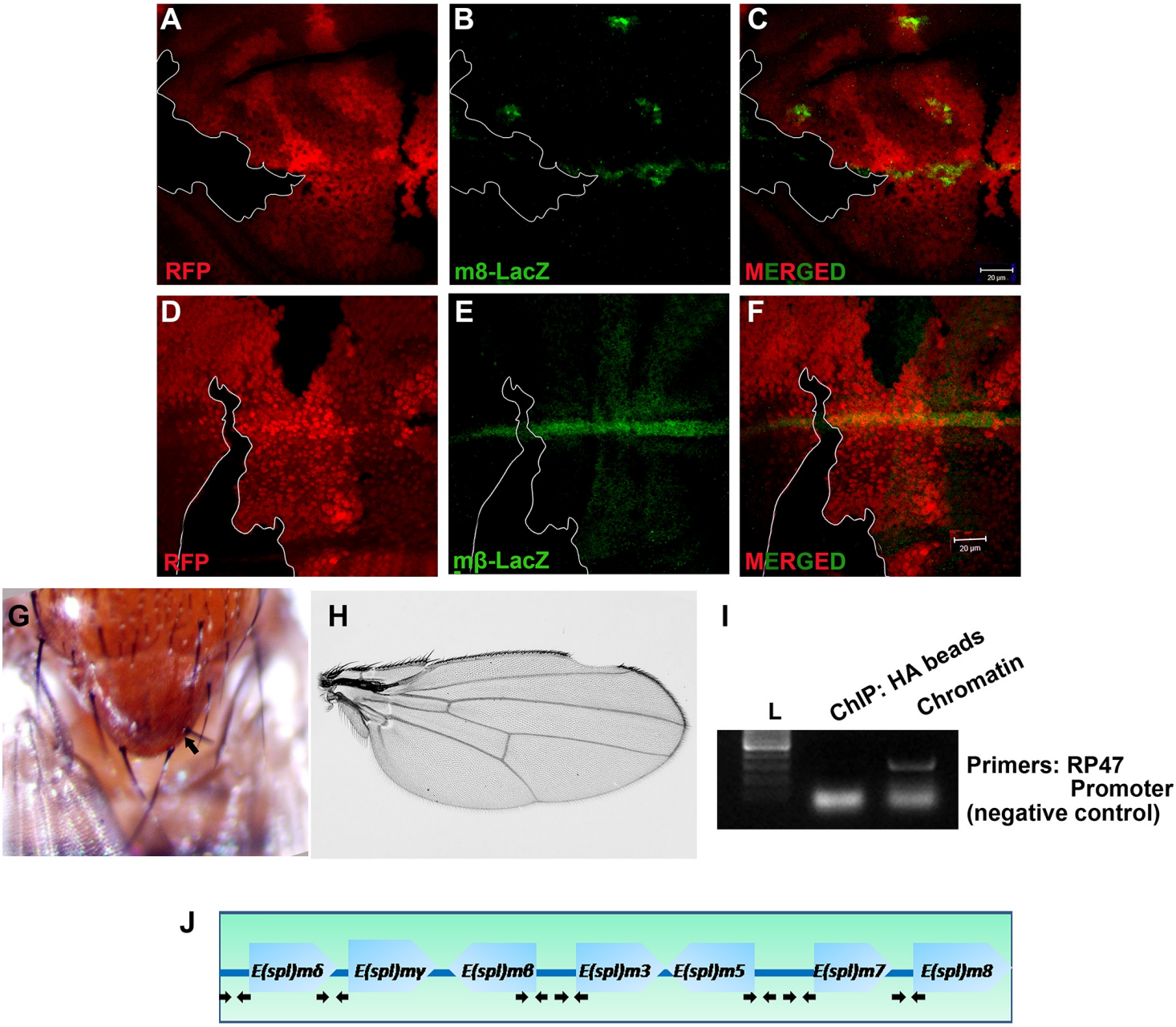


**Figure S5: *htk* regulates Notch signaling activity. (A-F)** Loss-of-function clones of *htk* displayed reduced expression of *E(spl)* complex genes. **(A, D)** *htk* mutant somatic clones were marked by absence of RFP expression. **(B, E)** The LacZ reporter stocks were used to verify *E(spl)m8* and *E(spl)mβ* expression (shown in green)**.** Third column images are merges of those in first and second columns. The expression of Notch downstream targets, *E(spl)m8* **(A-C)** and *E(spl)mβ* **(D-F)** was significantly reduced in *htk* loss-of-function clones. Scale bar, 20 µM. **(G-H)** Adults developed from larvae containing *htk* loss-of-function somatic clones, displayed various developmental defects such as increased scutellar bristles **(arrow, G),** notching at wing margin **(H),** etc. These phenotypes are also Notch loss-of-function phenotypes. **I.** Agarose gel electrophoresis image for negative control showing that Htk could not immunoprecipitate promoter of *RPS 49* gene. PCR using primers specific for promoter of *RPS 49* gene shows no positive amplification from template DNA fragments which was immunoprecipitated with Htk protein (Lane2). Chromatin samples before immunoprecipitation contain all the genomic DNA fragments, and were used for positive control (Lane 3). **J.** Schematic picture representing the localization of the primers used for ChIP experiment.

A

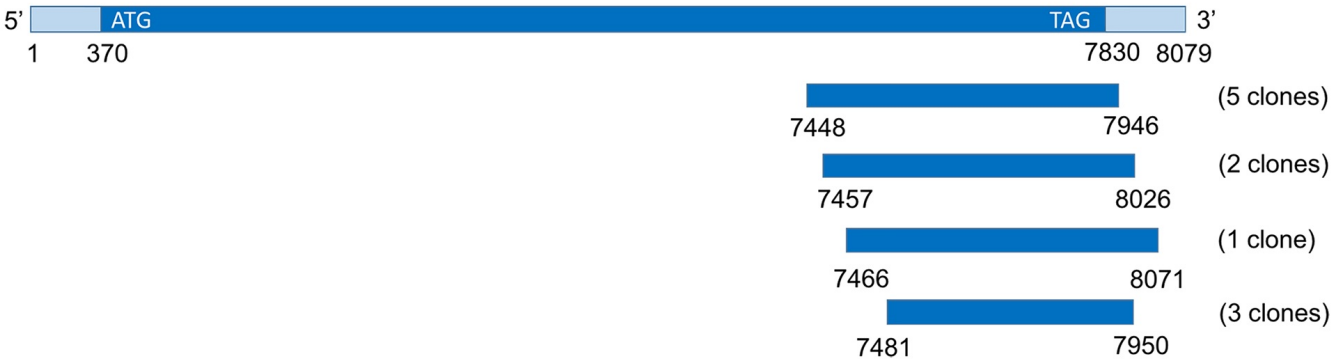


B

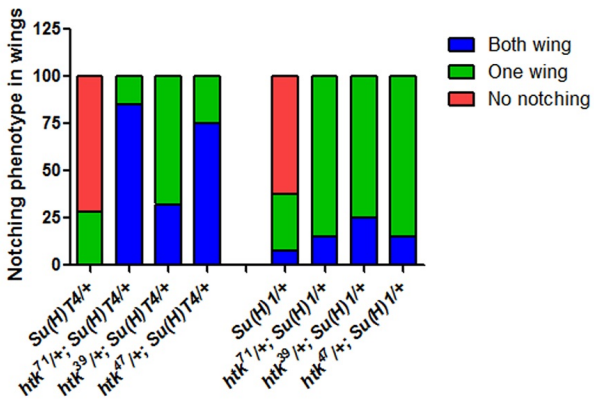


C

| Genotype | Phenotypes (%) |
|---|---|
| *+/+; ap-GAL4/+; UAS-htk-RNAi/+* | Extra vein material near 2nd Cross Vein : 46%<br>Defect in 2nd cross vein : 60%<br>Extra row of bristles near wing margin : 34%<br>1st vein defective : 100%<br>Patch of disorganized tissue at the tip of the vein : 60%<br>Blisters in wing : 14%<br>wings directed outward and upward : 100%<br>Increased scutellar bristles : 72% |
| *+/+; MS1096 –GAL4/+; UAS-htk-RNAi/+* | Extra row of bristles near wing margin : 89%<br>Patch of disorganized tissue at the tip of the vein : 72%<br>Defect in 1st cross vein : 52% |
| *+/+; +/+; C96 -GAL4 /UAS-htk-RNAi* | Defect in 1st cross vein : 44%<br>Extra vein : 12%<br>Unusual bristle pattern : 39%<br>Patch of disorganized tissue at the tip of the vein : 39% |
| *+/+; ptc-GAL4 /+;UAS-htk-RNAi/+* | Defect in 1st cross vein : 75%<br>Patch of disorganized tissue at the tip of the vein : 52.5%<br>Extra vein material near cross vein : 13%<br>1st cross vein very short and reduced intervein distance between L3-L4 : 100% |
| *+/+; +/+; dpp-Gal4/UAS-htk-RNAi* | Extra vein material near 2nd cross vein : 7.14%<br>Patch of disorganized tissue at the tip of the vein : 49%<br>Double 1st cross vein : 4% |
| *+/+; en-GAL4/+; UAS-htk-RNAi* | mis-oriented bristles and thinner wing blade in posterior region of wings : 75% |
| *+/+; ey-GAL4/+; UAS-htk-RNAi* | Reduced eye size :100% |

D

| Genotype | Phenotypes (100%) |
|---|---|
| *+/+; ap-GAL4/+; UAS-HA-htk/+* | • loss of scutellar bristles<br>• reduced size of scutellum<br>• severe wing blisters |
| *+/+; en-GAL4 /+; UAS-HA-htk/+* | • bending of third wing vein<br>• thinner wing blade<br>• incomplete fifth vein |
| *+/+; ey-GAL4 /+;UAS-HA-htk/+* | • loss of ommatidia |
| *+/+; +/+; GMR-Gal4/UAS-HA-htk* | • eye roughening |

**Figure S1: (A)** Schematic representation of the sequence range of 11 positive yeast two-hybrid clones which overlapped with *htk* cDNA, when amino terminus of Notch-ICD (amino acids 1765–1895) was used as bait to screen 6x10$^6$ cDNAs from a *Drosophila* 0–24 h embryonic library. **(B)** Graph showing the frequency (number) of wing notching phenotypes observed in *Su(H)T4* and *Su(H)1* alleles individually and in trans-heterozygous combination with different *htk* alleles: *htk$^{71}$, htk$^{39}$, htk$^{47}$*. **(C)** Development defects induced by down-regulation of *htk* with a variety of GAL4 drivers, n=200. **(D)** Defects observed in wing and eye when ectopic expression of HA-*htk* was induced with a variety of GAL4 drivers, n=200. All phenotypes examined were 100% penetrant.

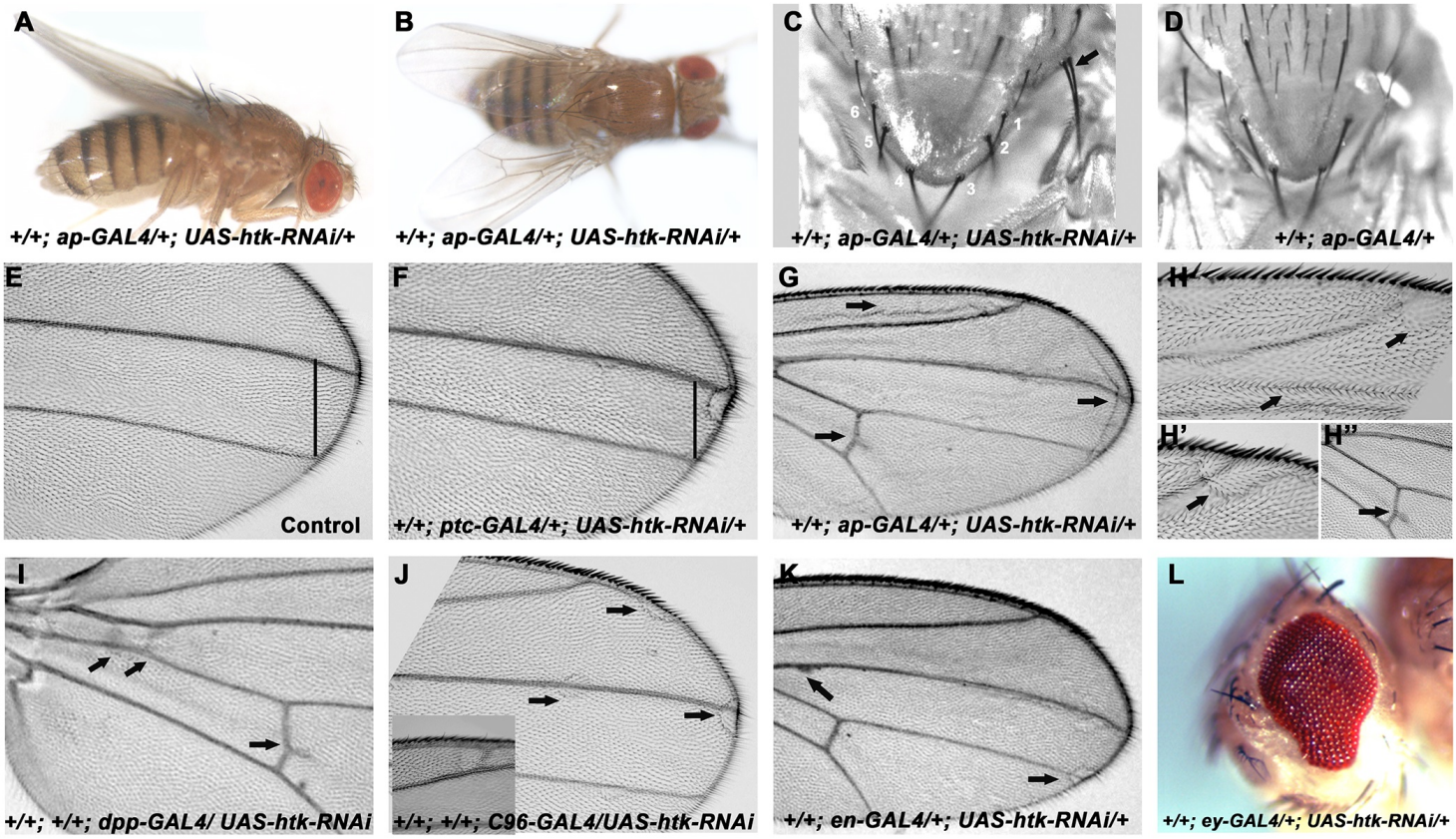


**Figure S2**: **Down-regulation of *htk* exhibits distinct phenotypes in *Drosophila* wings and eyes. (A-D, G)** *apterous-GAL4* driven *htk-RNAi* displayed upward (A) and outward (B) directed wings with extra rows of sensory bristles and vein material (arrow) in the wingblade (G), and increased scutellar bristles (C) compared to control (D). Similarly when *htk* was down-regulated at anterior-posterior boundary using *patched-GAL4* **(F)** and *dpp-GAL4* **(I),** at wing margin using using *C96-GAL4* **(J)**, in posterior compartment of wing using *engrailed-GAL4* **(K)**, and in the eye using *eyeless-GAL4* **(L)**, it resulted in reduced distance between L3 and L4 veins (black line) **(F)**, extra vein material (arrows) **(I)**, areas with thinner cuticle (arrows) **(J, K)** and reduced eye-size **(L)**, respectively. **(E)** Control adult wing displaying normal wing margin and longitudinal veins L1–L5. **(H-H")** High magnification images of wing showing extra row of bristles (H), area with thinner cuticle (H'), and extra vein material (H''). Several htk down-regulation phenotypes mimic Notch loss-of-function phenotypes.

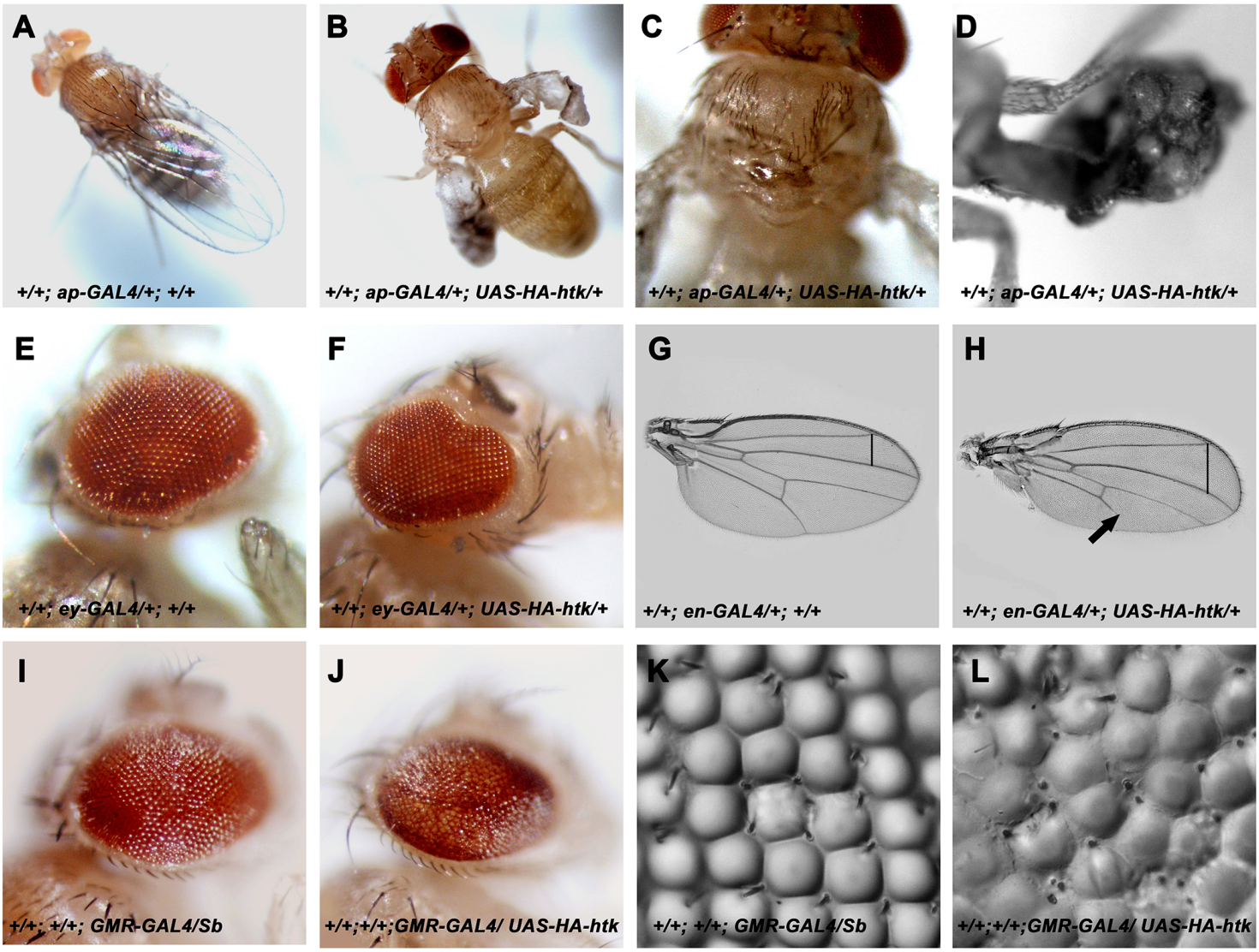


**Figure S3**: **Over-expression of *htk* resembles *Notch* gain-of-function phenotypes. (A-D)** Ectopic expression of *htk* driven by *apterous-GAL4* causes loss of scutellar bristles **(B, C)** and deformed wing **(B, D)** in comparison to only *apterous-Gal4/+* fly **(A)**. **(E,F)** *eyeless-GAL4* driven expression of *htk* in eye results in loss of ommatidia. **(G,H)** Over-expression of *htk* in posterior region of wing using *engrailed-GAL4* results in incomplete fifth vein and increased inter-vein distance between second and third vein. **(I, J)** Ectopic expression in adult eye using *GMR-GAL4* results in increased eye-roughening and loss of ommatidial bristles. **(K, L)** Nail polish imprint images of adult eye showing these eye phenotypes more clearly. Phenotypes showed 100% penetrance.

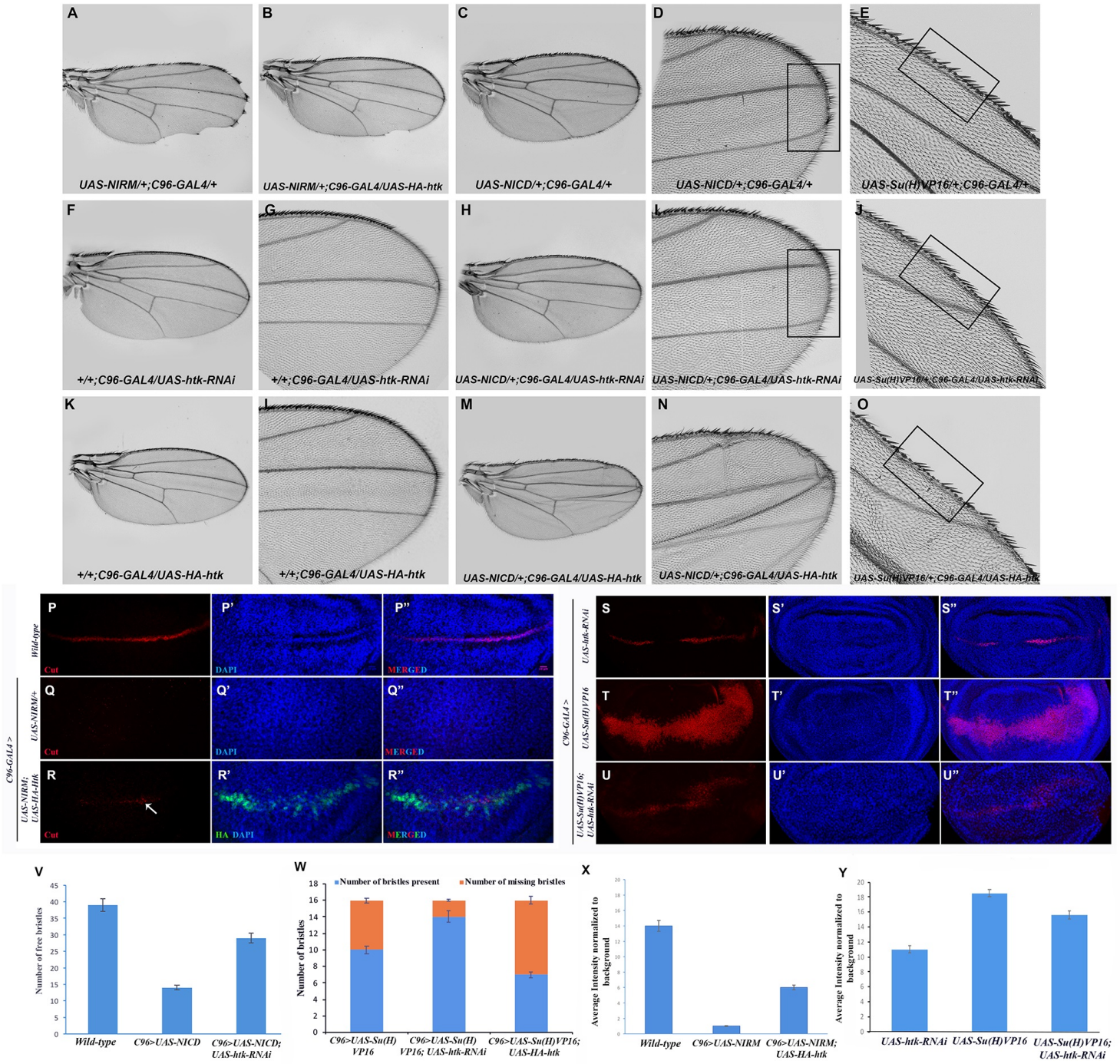


**Figure S4: Epistatic interactions of *htk* with Notch pathway.** *C96-GAL4* was used to drive the expression of different *UAS* lines at wing margin. **(A-O) Wing images showing epistatic and synergistic interactions between *htk* and *Notch* or *Su(H)VP16***. No notching or bristle irregularities were observed when *htk* was downregulated (F, G), or upregulated (K, L) at the wing margin. When the dose of *htk* was increased in *Notch* loss-of-function background, the wing notching phenotype caused by *Notch-RNAi* (A) was significantly rescued (B). Over-expression of *Notch* (C, D) and *Su(H)VP16* (E) at the wing margin resulted irregularities in wing bristle. This irregularity in bristle pattern was rescued when dosage of *htk* was reduced in this background (H-J). The irregularity in bristle localization was quantified by counting the number of free bristles in the same selected area of wing (n=10) expressing *Notch-ICD* alone and *Notch-ICD* along with *htk-RNAi* (boxed regions, 350µm length) **(V)**, and by counting the number of thick dorsal bristles present or absent in the same selected area of wing expressing *Su(H)VP16* alone and *Su(H)VP16* along with *htk-RNAi* (boxed region, 200µm length) **(W) [**error bars indicate standard error of the mean (n=3)]. The quantification is represented as the graph. Additionally, when *htk* along with *Notch* or *Su(H)VP16* were co-expressed, an increase in the wing margin irregularities was observed (M-O). All the phenotypes showed 100% penetrance (n=100). **(P-U'') Activity of Notch signaling was observed during epistatic interaction of *htk* with *Notch* and *Su(H)VP16***. Notch downstream marker, Cut was used to report the Notch signaling activity. DAPI marked the nuclei. The wild type Cut expression (P) was lost when Notch was reduced at dorso-ventral boundary of wing disc (Q). A rescue in the Cut expression was observed when *HA-htk* was over-expressed in the same background (R). (S-U'') Alternatively, ectopic expression of Cut caused by over-expression of *Su(H)VP16* (T) was partially rescued when *htk* was reduced in this background (U). Images in third column in both the panel are merged of images from first and second column. **(X, Y)** Quantification of Cut signal intensity at dorso-ventral boundary of wing disc is represented in the form of a graph. Cut signals are normalized to background signals, and values relative to controls are presented. Error bars indicate standard error of the mean (n=3). Figure D, G, I, L, N are higher magnification images of C, F, H, K, M, respectively. Scale bar, (P-U'') 10µm.

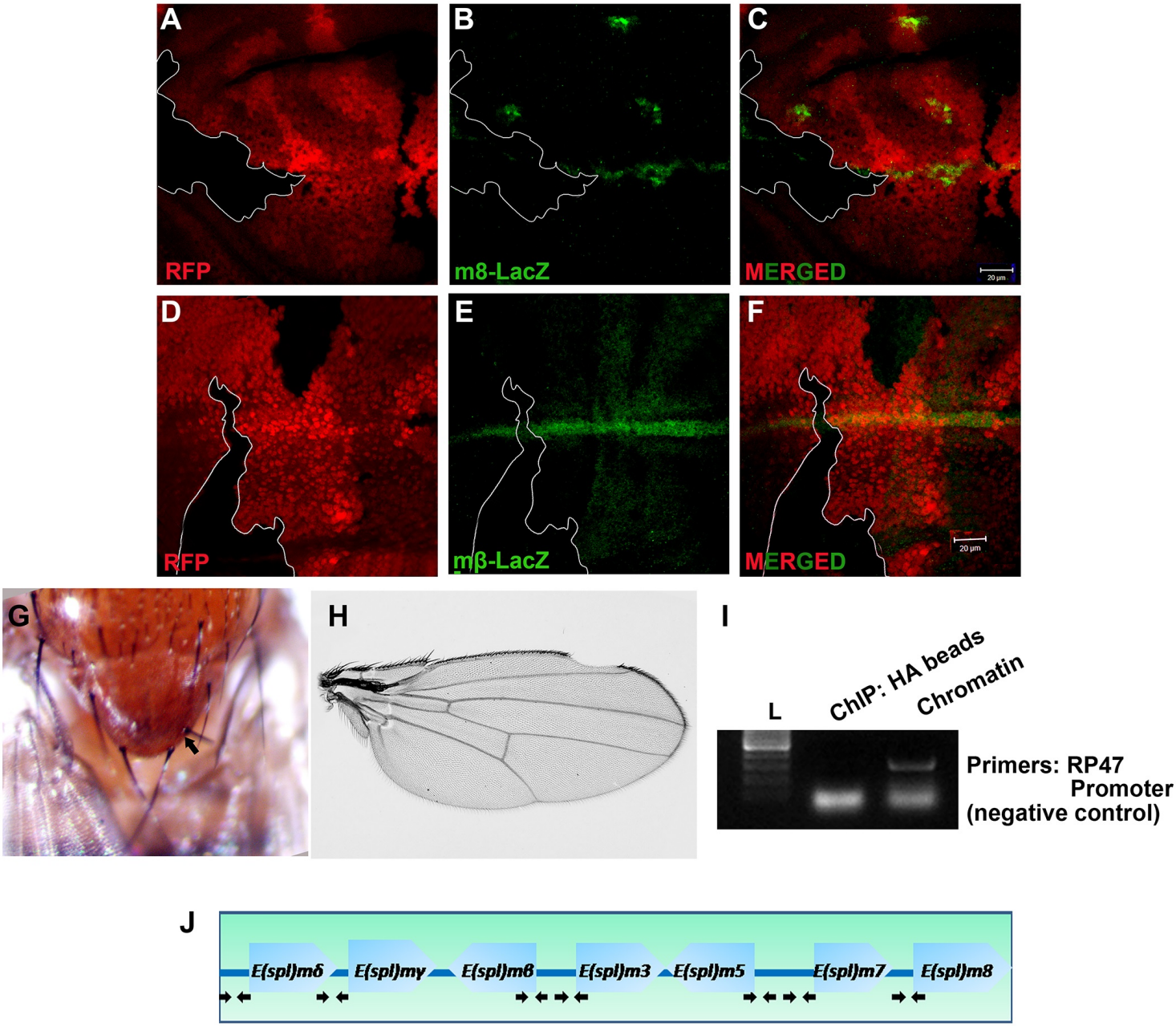


**Figure S5: *htk* regulates Notch signaling activity. (A-F)** Loss-of-function clones of *htk* displayed reduced expression of *E(spl)* complex genes. **(A, D)** *htk* mutant somatic clones were marked by absence of RFP expression. **(B, E)** The LacZ reporter stocks were used to verify *E(spl)m8* and *E(spl)mβ* expression (shown in green)**.** Third column images are merges of those in first and second columns. The expression of Notch downstream targets, *E(spl)m8* **(A-C)** and *E(spl)mβ* **(D-F)** was significantly reduced in *htk* loss-of-function clones. Scale bar, 20 µM. **(G-H)** Adults developed from larvae containing *htk* loss-of-function somatic clones, displayed various developmental defects such as increased scutellar bristles **(arrow, G),** notching at wing margin **(H),** etc. These phenotypes are also Notch loss-of-function phenotypes. **I.** Agarose gel electrophoresis image for negative control showing that Htk could not immunoprecipitate promoter of *RPS 49* gene. PCR using primers specific for promoter of *RPS 49* gene shows no positive amplification from template DNA fragments which was immunoprecipitated with Htk protein (Lane2). Chromatin samples before immunoprecipitation contain all the genomic DNA fragments, and were used for positive control (Lane 3). **J.** Schematic picture representing the localization of the primers used for ChIP experiment.

**Table S1. Primers for RT-qPCR**

| |
|---|
| mβ_RT_Fw 5'- ACCGCAAGGTGATGAAGC -3' |
| mβ_RT_Re 5'- CTTCATGTGCTCCACGGTC -3' |
| mδ_RT_Fw 5'- ATGGCCGTTCAGGGTCAG -3' |
| mδ_RT_Re 5'- CCATGGTGTCCACGATG -3' |
| mγ_RT_Fw 5'- GTCCGAGATGTCCAAGAC -3' |
| mγ_RT_Re 5'- GACTCCAAGGTGGCAACC -3' |
| m3_RT_Fw 5'- ATGGTCATGGAGATGTCC -3' |
| m3_RT_Re 5'- GCACTCCACCATCAGATC -3' |
| m5_RT_Fw 5'- ATGGCACCACAGAGCAAC-3' |
| m5_RT_Re 5'-TGTCCATTCGCAGGATGG -3' |
| m7_RT_Fw 5'- GGCCACCAAATACGAGATG -3' |
| m7_RT_Re 5'- CAT CGC CAG TCT GAG CAA -3' |
| m8_RT_Fw 5'- GGAATACACCACCAAGACC -3' |
| m8_RT_Re 5'- CGCTGACTCGAGCATCTC -3' |

**Table S2. Primers for promoter regions**

| |
|---|
| m3_Fw 5’-GATCCAATCCGAAAGCCG-3’ |
| m3_Re 5’-CTAGTTCCCAGCCCTACT-3’ |
| m5_Fw 5’-GTGGTTGTCTGTGTGGAG-3’ |
| m5_Re 5’-GACCTGCTACCTGCGAACA-3’ |
| m7_Fw 5’-GCACGCATGTTCCGTTTG-3’ |
| m7_Re 5’-GGGAAACACTTTGCCCTC-3’ |
| m8_Fw 5’-GCCAATATGCCACATCCAC-3’ |
| m8_Re 5’-GGAACAGCTGCAACTTCG-3’ |
| mβ_Fw 5’-ACTTCGATCGGTTCCCAG-3’ |
| mβ_Re 5’-GAACTGGACAGTGAGTGC-3’ |
| mδ_Fw 5’-GCGGCACAATCCCAATAC-3’ |
| mδ_Re 5’-CTGGTTCCCACTTCCCT-3’ |
| mγ_Fw 5’-CACTCCGTTTACAAATCCCTG-3’ |
| mγ_Re 5’-GCTAGACCTTCGGTGATC-3’ |